Journal Pre-proof

Lithosphere thickness controls the extent of mantle melting, depth of melt extraction and basalt compositions in all tectonic settings on Earth – A review and new perspectives

Yaoling Niu

Please cite this article as: Y. Niu, Lithosphere thickness controls the extent of mantle melting, depth of melt extraction and basalt compositions in all tectonic settings on Earth – A review and new perspectives, *Earth-Science Reviews* (2021), https://doi.org/10.1016/j.earscirev.2021.103614

Lithosphere thickness controls the extent of mantle melting, depth of melt extraction and basalt compositions in all tectonic settings on Earth – A review and new perspectives

Yaoling Niu [1,2,3]

[1] China University of Geosciences, Beijing 100083, China
[2,*] Department of Earth Sciences, Durham University, Durham DH1 3LE, UK
[3]. Qingdao National Laboratory for Marine Science and Technology (Marine Geology), Qingdao 266061, China

*Correspondence:
Yaoling Niu (yaoling.niu@durham.ac.uk)

Highlights:

- First order compositional systematics of mid-ocean ridge basalts (MORB), volcanic arc basalts (VAB), ocean island basalts (OIB) and basalts in continental interiors (CIB) vary a function of lithosphere thickness
- In all settings, lithospheric thickness controls the extent of mantle melting, depth of melt extraction and basalt compositions, i.e., the *lid effect*
- Basalts have no memory of initial depth of mantle melting, at least for olivine making elements (i.e., Si, Mg and Fe), because of effective and efficient melt-solid equilibration in the decompression melting mantle
- Thermobarometers using basalt-olivine equilibria provide no information on initial depth of melting and mantle potential temperature, but record the depth of melt extraction at the base of the *lithospheric lid*
- The strength and thickness of lithosphere controls whether a mantle plume can surface or not and large igneous provinces (LIPs) manifest thin or thinned lithosphere at the time of volcanism
- The *paradigm* of mantle potential temperature control on basalt composition needs revision

Table of Contents

ABSTRACT

Basalts and basaltic rocks are the most abundant igneous rocks on the earth and their petrologic and geochemical studies have formed our knowledge base on the thermal structure and composition of the mantle with which we have developed workable models on the chemical differentiation of the earth. All this would not have been possible without innovative and painstaking experimental petrology on mantle peridotite melting, basaltic magma generation and evolution largely done in the period of 1960s -1980s. However, the ~ 30 year lively debate on the nature of "primary magma" among experimental petrologists and the petrology community during this time had inadvertently shelved the development of consensus models on mantle melting in the context of plate tectonics. Continued experimental petrology in parallel with worldwide sampling and study of mid-ocean ridge basalts (MORB) brought about new insights, culminating with a model in 1980s that mantle potential temperature (T_{MP}) variation controls the extent and pressure of mantle melting and basalt compositions. The tenet of this model is that hotter rising mantle begins to melt deeper and thus has greater decompression depth interval to melt more with the melt having the petrological signature of higher extent and pressure of melting than cooler mantle. This model has gained wide acceptance in MORB studies and has also been invoked in the study of intra-plate basalts in ocean basins and in continental settings. Basalt generation above subduction zones, on the other hand, has been generally accepted as resulting from slab-dehydration induced mantle wedge melting since early 1980s, but recent studies also advocate mantle temperature variation as the primary control on the extent of mantle wedge melting. All these views with laudable merits have formed a *paradigm* on mantle melting and basaltic magmatism. In this paper, I review the historical developments towards this paradigm and demonstrate in simple clarity that it is the lithosphere thickness, *not* T_{MP}, that controls the extent of mantle melting, depth of melt extraction and basalt compositions, i.e., the *lid effect*. The lithospheric *lid* caps the rising melting mantle, thus limiting the extent of decompression melting and equilibrium pressure/depth of melt extraction, which is well registered in the compositions of MORB, intra-plate ocean island basalts (OIB), volcanic arc basalts above subduction zones (VAB) and basalts in continental interiors (CIB). Hence, lithosphere thickness is the *governing variable* controlling mantle melt compositions in all tectonic settings on earth. Major element compositions (e.g., Si-Mg-Fe) of erupted basalts have no memory of initial depth of melting because of effective and efficient melt-solid (e.g., olivine [Mg,Fe]$_2$SiO$_4$) equilibration in the rising meting mantle. Therefore, basalt-olivine based thermobarometry, albeit useful, supplies no information on T_{MP}. It is also the lithosphere thickness that controls whether "mantle plumes" can surface or not and the large igneous provinces (LIPs) serve as effective manifestations for thin or thinned lithosphere at the time of emplacement. This new understanding based on global observations, well-understood experimental petrology and rigorous analysis is fundamental and requires a major change to the current *paradigm*.

Introduction

Basalts and basaltic rocks are the most abundant igneous rocks on the earth and their petrology and geochemistry have been used to infer the thermal structure and composition of the mantle and to research the chemical differentiation of the earth (e.g., Zindler and Hart, 1986; Hofmann, 1988, 1997; Wyllie, 1988a,b; Sun and McDonough, 1989; McDonough and Sun, 1995; Herzberg and O'Hara, 2002; Herzberg et al., 2007; Putirka, 2005, 2008; Lee et al., 2009). However, it was unclear until 1960s that the mantle consists of peridotites whose partial melting produces basaltic magmas thanks to experimental petrology (e.g., Ringwood, 1962; Green and Ringwood, 1963, 1964, 1967, 1970; O'Hara and Yoder, 1963, 1967; O'Hara, 1963, 1965, 1967, 1968a, 1968b, 1970; Green, 1968; Kushiro, 1968,1973; Presnall, 1979). Yet debate continued on what may actually cause the partial melting until 1970s when decompression melting became gradually accepted as the important mechanism (Carmichael et al., 1974; Yoder, 1976) although this concept was conceived in 1950s (Verhoogen, 1954) and developed further by comparing natural basalts with experimental melts in 1960s (Green and Ringwood, 1967). These early experimental studies have formed a solid foundation for many aspects of our present-day knowledge on basalt genesis in terms of peridotite compositions, pressure and temperature conditions, effect of water and phase equilibria, but had not developed into a consensus paradigm in the context of plate tectonics because of the ~ 30 year lively debate on the nature of "primary magma" among experimental petrologists and in the basalt petrology community, i.e., (1) picritic liquids formed by 20-30% melting at pressures of ~ 20-30 kbar or (2) tholeiitic liquids formed by 10-12% melting at shallow depths (~ 10 kbar) (see review by Niu, 1997, pages 1061-1062).

Continued experimental petrology (e.g., Green, 1971, 1973; Jaques and Green, 1980; Falloon and Green, 1987, 1988; Falloon et al., 1988) in parallel with worldwide sampling and study of mid-ocean ridge basalts (MORB; see sampling expeditions and data given in Klein and Langmuir, 1987, 1989; Brodholt and Batiza, 1989; Niu and Batiza, 1993) brought about new insights, culminating with theoretical models in 1980s that mantle potential temperature (T_{MP}) variation controls the extent and pressure of mantle melting (Dick et al., 1984; McKenzie, 1984; Klein and Langmuir, 1987, 1989; McKenzie and Bickle, 1988; Niu and Batiza, 1991; Kinzler and Grove, 1992; Langmuir et al., 1992). The most influential model by Langmuir and co-authors (Klein and Langmuir, 1987, 1989; Langmuir et al., 1992; Gale et al., 2014; Dalton et al., 2014) details that hotter rising mantle begins to melt deeper, has taller melting column to melt more, produces thicker crust and shallower ridge depth with the melt having the signature of higher extent and pressure of melting. All this is opposite for ridges above colder mantle. The same ideas have been invoked in the study of intraplate magmatism in ocean basins (e.g., Yang et al., 2003; Putirka, 2008; Armitage et al., 2008; Sager et al., 2016; Jennings et al., 2019) and in continental interiors (e.g., Li et al., 2008; Wang et al., 2008; Plank and Forsyth, 2016).

This model with laudable merits has thus become a *paradigm* on mantle melting and basaltic magmatism, i.e., *T_{MP} variation controls the extent of mantle melting and basalt compositions*. However, this model has basic problems (Niu, 1997, 2004): [1] the petrological parameter used to infer the initial depth of melting (i.e., Fe_8 = FeO wt.% at MgO = 8.0 wt.%) is invalid (see Niu and O'Hara, 2008; Niu, 2016a); [2] the assumption that decompression melting continues all the way to the Moho ignores the presence and effect of conductive

thermal boundary layer (CTBL) atop the mantle (Niu and Hékinian, 1997; Niu, 2016a); and [3] erupted basalts have no memory of initial depth of melting, but preserve the signature of final depth of melt equilibration at the base of the CTBL (Niu, 2016a). Given the fundamental importance of the basalt problem in addressing issues of mantle dynamics in a global context, it is time to review the progress in the study of basalt petrogenesis, which I have been involved in and my research has dedicated to over the past 30 years. Basalt compositions are determined by [1] fertile mantle source compositions, [2] conditions of mantle melting, and [3] complex magma differentiation processes largely in crustal magma chambers before eruption. In this review, I focus on [2] although [1] can have deterministic effect on [2] (Niu et al., 2001; Niu and O'Hara, 2008). I demonstrate in simple clarity that the first order global MORB systematics is a consequence of the lithospheric thickness variation, termed *lid effect*. The lid effect is well registered in the compositions of basalts in all tectonic settings, not only in MORB, but also in intra-plate ocean island basalts (OIB), volcanic arc basalts above subduction zones (VAB) and basalts in continental interiors (CIB). It is also the *lithospheric lid* that controls whether "mantle plumes" can surface or not and large igneous provinces (LIPs) serve as effective manifestations for thin or thinned lithosphere at the time of their emplacement. Because erupted basalts, which only record the final depth of melting and melt equilibration at the base of the CTBL, have no memory of initial depth of melting in terms of olivine-making elements SiO_2, FeO and MgO, basalt-olivine-based thermobarometry, albeit useful, provides no information on the initial depth of mantle melting and T_{MP}.

The unifying *lid effect* as the governing variable that controls the extent of mantle melting and basalt composition in all tectonic settings on earth demands a fundamental change on the current *paradigm* in order to use basalt petrogenesis as a tool to advance our understanding of global mantle dynamics. In the following I start by reviewing basic concepts that may not be well connected for many when considering basaltic magmatism in terms of experimental petrology and in the context of global tectonics. I will then show the data and guide the reader to appreciate the lithosphere thickness variation, the *governing variable*, that controls the compositions of basalts in all tectonic settings on earth. To ease the readability, all the technical details are given in relevant figure captions.

Basic geological concepts relevant to mantle melting and magma generation

2.1 Why basalt magmas erupt where they do?

Fig. 1 shows the familiar Earth cross section with the internal layered structure and seismic P-wave and S-wave velocity variation as a function of depth. The equations in (a) state that the material properties such as density (ρ), bulk modulus (K) and shear modulus (μ) determine P-wave (V_P) and S-wave (V_S) seismic velocities. The observation that $V_S = 0$ because of $\mu = 0$ tells us that the outer core is entirely liquid. By inference, the fact that at no depth in the mantle $V_S = 0$ but $V_S \gg 0$ states clearly that the Earth's mantle is entirely solid with no volumetrically significant melt anywhere and at any depth. Hence, in a global context, mantle melting with magma formation is a highly localized shallow phenomenon. These highly "localized" localities of mantle melting are well understood in the framework of plate tectonics to be associated with plate boundaries (Fig. 2). For example, at divergent boundaries such as mid-ocean ridges, mantle melting produces mid-ocean ridge basalts (MORB) that create the ocean crust, which covers about two-thirds of the earth's surface (e.g., Macdonald, 1982). At convergent boundaries such as the Izu-Bonin-Mariana island arcs, mantle wedge melting produces volcanic arc basalts (VAB) (e.g., Perfit et al., 1980; Gill, 1981; Arculus, 1981; Tatsumi and Eggins, 1995), which is thought to be responsible for continental crust accretion (e.g., Taylor, 1967; Arculus, 1981) despite the debate (Niu et al., 2013). However,

there is also widespread basaltic magmatism in plate interiors away from plate boundaries such as Hawaiian volcanoes. These within-plate basaltic volcanoes have thus been considered as mantle melting "anomalies" associated with anomalously hot mantle or "hotspots" (Wilson, 1963), which are later interpreted as the surface expressions of deep-rooted mantle plumes derived from the lower mantle or core-mantle boundary (Morgan, 1971). Whether mantle plumes exist or not in the earth has been the subject of hot debate (Anderson, 2004; Foulger and Natland, 2003; Davies, 2005; Foulger, 2005, 2010; Campbell, 2005; Niu, 2005a; Campbell and Davies, 2006; Green and Falloon, 2005, 2015), which is beyond the theme of this review. Regardless of tectonic settings, mantle melting occurs only if the mantle peridotites are placed at or above the solidus as illustrated in Fig. 3.

2.2 Mechanisms of mantle melting

Fig. 3 illustrates, in pressure-temperature (P-T) space, the way in which mantle melting may occur. The concepts of solidus, conductive geothermal gradient, convective geothermal gradient (i.e., the adiabat or adiabatic geotherm) and mantle potential temperature (T_{MP}) are all self-explained. The effect of minute volatiles on the solidus is insignificant for volumetrically important magma generation and can thus be neglected here for clarity (Niu and Green, 2018). The concepts that need clarifying are as follows:

[1] The mantle peridotite below the solidus is always solid, and it can partially melt only when placed onto or above the solidus.

[2] The slope of the adiabat is less steep than that of the solidus (i.e., $dT/dP_{[ADIABAT]} < dT/dP_{[SOLIDUS]}$), making decompression melting possible because the adiabatically rising mantle can cross over the solidus at P_O (see below).

[3] Adiabatically rising mantle with higher T_{MP} (e.g., $T_{MP[hot]}$ beneath intra-place settings; Fig. 3d) intersects the solidus and begins to melt deeper (P_O) than the rising mantle with lower T_{MP} (e.g., $T_{MP[normal]}$ beneath ocean ridges (Fig. 3c).

[4] The lithosphere is the conductive thermal boundary layer (CTBL), whose slope $dT/dP_{[CONDUCTIVE]}$ decreases with increasing lithosphere thickness.

[5] Decompression melting begins when the adiabatically rising mantle intersects the solidus at P_O (see [3] above) but ends when the melting mantle encounters the base of the lithosphere at P_F, which is the base of the CTBL and is the same as the lithosphere-asthenosphere boundary (LAB; Niu and Green, 2018). The extent of melting (F) is thus proportional to the decompression depth interval, i.e., $F \propto P_O - P_F$, which is the case for MORB, OIB, VAB and CIB (see below).

[6] Mantle upwelling beneath ocean ridges is a passive response to plate separation, i.e., plate separation creates a gravitational void to allow the hot and buoyant asthenosphere to rise (McKenzie and Bickle, 1988).

[7] Mantle upwelling beneath intra-plate settings is considered active or dynamic because of the hot and buoyant "mantle plumes" (e. g., Sleep, 1990; Davies, 1999).

[8] Because the solidus is a material property, its position and topology in P-T space vary, depending on the compositions, especially the effect of H_2O-dominated volatiles (Fig. 3e; also see Niu and Green, 2018 and Fig. 14c below). The parcel of mantle indicated with a blue open star at that depth in Fig. 3c will remain solid without melting, but introduction of water into the mantle will change the solidus into the wet solidus as shown in Fig. 3e, where the blue open star will become located above the wet solidus, causing melting to occur. Hence, VAB above subduction zones are understood as slab-dehydration induced mantle wedge melting or fluid flux melting, which is consistent with the VAB geochemistry in having elevated abundances of H_2O and H_2O-soluble chemical elements although decompression facilitated melting must also

be at work (see Section 5 below).

2.3 Do basalts record mantle melting conditions?

Our current understanding of mantle melting and basalt magma formation owes a great deal to the experimental petrology as discussed above. The work by Jaques and Green (1980) is particularly instrumental by demonstrating for the first time how the compositions of mantle melts vary systematically as a function of fertile mantle compositions and the extent and pressure of melting, which laid the foundation for a number of petrological models for MORB petrogenesis (e.g., Klein and Langmuir, 1987; McKenzie and Bickle, 1988; Niu and Batiza, 1991; Kinzler and Grove, 1992; Langmuir et al., 1992). Fig. 4 shows major element compositions of primary MORB melts produced by decompression polybaric melting using one of these models (Niu, 1997) improved upon by incorporating diamond-aggregate constrained higher-pressure experimental melts (Hirose and Kushiro, 1993; Baker and Stolper, 1994). These models well capture the experimental melt compositions in terms of fertile mantle peridotite composition and the extent and pressure of melting, but their direct application to actual polybaric decompression mantle melting is not straightforward because the model melts represent the integrated melt compositions without considering continued melt-solid equilibration during the P_O-to-P_F decompression melting process whereas the erupted basalts do record such equilibration. This is particularly important for SiO_2, FeO and MgO because they are sensitive to the pressure of melt-solid equilibration and because the equilibration is effective and efficient, controlled by olivine ($[Mg,Fe]_2SiO_4$), which is the most abundant mineral (> 55 wt.%) in the melting mantle. On the other hand, elements such as Na_2O (also incompatible elements such as TiO_2, P_2O_5, K_2O, K_2O/TiO_2) and CaO/Al_2O_3 are incompatible in olivine and are thus insensitive to the melt-solid equilibration. Consequently, the erupted basalts are expected to have the signatures of the extent of melting (see Na_2O and CaO/Al_2O_3 in Fig. 4) and final depth/pressure (P_F) of melt-solid equilibration or melt extraction if preserved (see below).

2.4 Basalts have no memory of initial depth of melting (i.e., P_O) in terms of SiO_2, MgO and FeO

Although it is conceptually apparent that hotter rising mantle intersects the mantle solidus deeper (Fig. 3) and the melt would have the compositional signature of higher pressure of melting (i.e., higher MgO, FeO and lower SiO_2; Fig. 4) than cooler mantle. This is unlikely to be true in practice because of the continued and inevitable melt-solid equilibration during the P_O-to-P_F decompression melting. The pressure signature in basalts, if recorded and discernable, would be the final depth of melting (P_F), which is the depth of melting cessation and melt extraction (Niu, 1997, 2016a). This can be illustrated through Fig. 5 using the well-understood ocean ridge mantle melting processes (Niu, 1997, 2004, 2016a).

Fig. 5 shows plate separation induced passive mantle upwelling and decompression melting beneath ocean ridges. The decompression melting begins when the upwelling mantle intersects the solidus at P_O (corresponding to $T_O \propto T_{MP} = T_O - P_O * 1.8$ (°C); Niu and O'Hara, 2008), continues in the melting region ① and stops at P_F (corresponding T_F) capped by the CTBL (region ②). Because of the buoyancy contrast, the melt (red-arrowed dash lines) is extracted from the residue (blue-arrowed think lines) to form the ocean crust. The residue contributes to the new accretion of the mantle lithosphere, which, when tectonically exposed on the seafloor, is sampled as abyssal peridotites (Dick et al., 1984; Dick, 1989; Niu, 1997; 2004). Mantle melting is considered to be close to fractional polybaric and the

decompression melting mantle would have very small melt porosity (or melt retention), widely believed to be $<< 1\%$ (e.g., McKenzie, 1985; Johnson et al., 1990; Langmuir et al., 1992; Spiegelman and Elliott, 1993; Lundstrom et al., 1995; Sims et al., 2002). To be conservative, we can assume that in the P_O-to-P_F decompression melting region ①, there exists 1-2% melt retention (Niu, 1997) in close physical contact with 98-99% solid matrix dominated by olivine ($[Mg,Fe]_2SiO_4$). Such small melt/solid ratio ensures effective and efficient melt-solid re-equilibration, at the very least for elements Si, Fe and Mg controlled by olivine. The 1000's of years of melting time is really long enough to ensure complete melt-solid re-equilibration that is readily achieved in 10's of hours in peridotite melting experiments. We thus cannot avoid the conclusion that erupted basalts have no memory of initial depth of melting (P_O) in terms of olivine-making elements Si, Fe and Mg, but can record the final depth of melting or melt-solid equilibration (P_F) at which the upwelling mantle encounters the CTBL, stops to melt and ends the above-mentioned melt-solid re-equilibration. It is therefore simply invalid to use Fe_8 as proxy for T_{MP} in discussing mantle melting (see Fig. 4 and below). This analysis based on ocean ridge mantle melting applies to mantle melting in all other tectonic settings because there always exist CTBLs that cap the decompression melting (see Sections 3-6 below). It is necessary to emphasize in this context that fractional melting is equilibrium (*not* disequilibrium) melting, and the smaller the melt retention (i.e., melt porosity; e.g., $<< 1-2\%$) is, the more efficient in attending equilibrium. By definition, in the process of fractional melting, the melt will leave the residue immediately as soon as it is produced no matter how small amount and at what depth in the melting region ①, but such melt must escape from ①, during which melt-olivine equilibrium is inevitable for olivine-making elements Si, Mg and Fe although this may not apply to chemical elements incompatible in olivine.

Hence, erupted basalts have no memory of the initial depth (P_O) of melting in terms of Si, Mg and Fe, and thus provide no information on T_O and T_{MP}. Therefore, the basalt-olivine-based thermobarometry, albeit useful, has no significance when discussing T_{MP}. Because basalts can record the final depth of melting (P_F), the basalt-olivine-based thermobarometry can thus provide the information on P_F and CTBL thickness at the time of basaltic volcanism. It is important to note, while there exists CTBL beneath ocean ridges and its thickness increases with decreasing spreading rate (Niu, 1997, 2004, 2016a; Niu and Hékinian, 1997a), MORB may not even record the information about P_F. This statement is significant because abyssal peridotites, which are considered as sub-ridge mantle melting residues, are not simple melting residues, but contain excess olivines and elevated abundances of incompatible elements, ascertaining the fact of MORB melt cooling and olivine crystallization as well as melt refertilization during ascent through the advanced residues in the CTBL (Niu, 1997, 2004; Niu and Hékinian, 1997b; Niu et al., 1997). Hence, MORB melts have varying re-equilibration histories in the CTBL at varying depth shallower than P_F. Therefore, using MORB SiO_2, FeO and MgO (in whatever corrected forms such as Si_8-Fe_8, Si_{90}-Fe_{90}-Mg_{90}, Si_{72}-Fe_{72}-Fe_{72}) to discuss P_O, T_{MP} and mantle melting processes is invalid and has no significance (Niu, 2016a).

The *lid-effect* on mantle melting at *mid-ocean ridges* and MORB petrogenesis

The most referenced hypothesis on MORB magmatism at present is the work by Langmuir and co-workers (Klein and Langmuir, 1987, 1989; Langmuir et al., 1992). After Dick et al. (1984), Klein and Langmuir (1987) (abbreviated as KL87) showed correlated variations of MORB Fe_8 and Na_8 (i.e., FeO wt.% and Na_2O wt.% values corrected for fractionation to MgO

= 8 wt.%) with ridge axial depth on a global scale. They interpreted these correlations, following the experimental data of mantle peridotite melting (Jaques and Green, 1980), as reflecting varying extent and pressure of mantle melting in response to mantle solidus temperature variation of up to 250 K. This hypothesis profoundly influenced my PhD study on MORB magmatism although I focused on possible controls of ridge spreading rate variation (Niu, 1992). My one-year postdoctoral experience and a co-authored paper (Niu et al., 1997) with Charles Langmuir further motivated my continued enthusiasm on MORB petrogenesis. My subsequent research has demonstrated that the KL87 interpretation is fundamentally in error (Niu, 1997, 2016a; Niu and Hékinian, 1997a; Niu and O'Hara, 2008) despite its popular reference and influence.

3.1 The merit and errors of KL87 on global MORB petrogenesis

Langmuir et al. (1992) further elaborated quantitatively that the global MORB Fe_8 variation can be used to calculate the mantle solidus temperature ($T_O \approx T_{MP}$). Fig. 6 summarizes the ideas and errors of KL87. By interpreting the inverse correlation of ridge segment averaged MORB Fe_8 with ridge depth and the positive correlation of MORB Na_8 with ridge depth (Fig. 6c), KL87 states that MORB erupted at shallow ridges represent hot mantle that begins to melt deeper with higher extent of melting whereas MORB erupted at deep ridges reflect cooler mantle that begins to melt shallower with lower extent of melting, resulting in thicker crust beneath shallow ridges than beneath deep ridges (Fig. 6a,b). While this interpretation is simple and attractive, the fundamental assumptions are in error (Niu, 1997, 2004, 2016a; Niu and Hékinian, 1997a; Niu and O'Hara, 2008):

[1] The assumption that decompression melting continues all the way to the Moho ignores the near-seafloor cooling and thus ignores the presence and effect of the CTBL.

[2] The assumption that MORB mantle has uniform major element compositions neglects the effect of mantle source heterogeneity on the observed MORB chemistry.

[3] The assumption that FeO (or Fe_8) in MORB melts directly indicates the initial depth of mantle melting ignores the inevitable melt-solid equilibration in the melting mantle (see Fig. 5 and above). Hence, the calculated P_O, T_O and T_{MP} using the single variable Fe_8 have no significance (Fig. 6).

[4] The use of MORB Fe_8 corresponding to variably evolved MORB melts with Mg# = 0.56 – 0.68 to discuss mantle melting processes, violates basic petrological principles; MORB melts with Mg# ≥ 0.72 in equilibrium with mantle olivine of Fo_{90} can be used to discuss mantle processes (Niu and O'Hara, 2008). This simple and objective analysis further substantiates that Fe_8-based calculations for P_O, T_O and T_{MP} have no significance. Note that Gale et al., 2014) re-corrected the data to show $Fe_8 = Fe_{90}$ (MORB melt in equilibrium with mantle olivine Fo_{90}), but this re-correction is entirely flawed as illustrated in simple clarity in Fig. 3 of Niu (2016a).

[5] Therefore, the conclusion that global ocean ridge T_{MP} variation (up to $\Delta T_{MP} = 250$ K) controls the initial depth/pressure and extent of melting is entirely flawed and misguiding.

One may wish to relate MORB Na_8 to modal clinopyroxene (Cpx) in spatially related abyssal peridotites (AP; Fig. 7a) as evidence in support of T_{MP} control on the extent of mantle melting because both are expected to decrease with increasing extent of melting towards beneath shallow ridges (see Niu et al., 1997). However, this correlation can be readily understood as inherited from the sub-ridge fertile mantle compositional variation reflecting previous melting and melt extraction histories with compositionally depleted (low Na_2O, low Cpx mode) and

physically buoyant mantle beneath shallow ridges (Fig. 7b; Niu, 2004, 2016a). The AP samples are from fracture zone walls 0.5 to 14 Ma old, yet the spatially associated basalts are from the present-day ridge axis (Dick et al., 2007). Despite the compositional complementarity between MORB (melt) and AP (residue), it is unlikely for the ~ 14 Ma old AP to be melting residues of the present-day MORB. Mantle temperature anomalies could be long-lived but will decay away with time toward increased ridge depths. Compositional anomalies (buoyant mantle beneath shallow ridges), however, will be long-lasting and will not decay away with time (Niu, 2016a).

3.2. The *lid-effect* on ridge mantle melting: Evidence from the correlation of MORB chemistry with spreading rate

With the understanding that ocean ridges are passive features and that sub-ridge mantle melting results from plate-separation induced asthenospheric upwelling and decompression (McKenzie and Bickle, 1988), it is thus logical to predict that plate separation rate must affect the extent of melting and MORB composition. This is because the rate of mantle upwelling is proportional to the rate of plate separation (Reid and Jackson, 1981; Phipps Morgan, 1987; Niu, 1992,1997). To test this hypothesis, Niu and Hékinian (1997a) analyzed the global MORB data and limited AP data available then and demonstrated that the extent of ocean ridge mantle melting increases with increasing plate spreading rate. Langmuir and co-workers denied this finding and stated that "*There is no correlation between the chemical parameters and spreading rate*" (Gale et al., 2014). In response to this denial, I used the updated global MORB data compiled by these authors and substantiated the finding done ~ 20 years earlier (Fig. 8a; Niu, 2016a). Fig. 8a shows that the average compositions of global MORB (in terms of K_2O/TiO_2 and Ca_{72}/Al_{72} corrected CaO and Al_2O_3 to Mg# = 0.72) vary systematically as a function of spreading rate and the extent of mantle melting increases (decrease in K_2O/TiO_2 and increase in Ca_{72}/Al_{72}) with increasing spreading rate. Such systematics is a straightforward consequence of the *lid-effect*, i.e., the CTBL thickness (region ②) control as illustrated in Fig. 8b. Fast mantle upwelling beneath fast-spreading ridges allows the adiabat to extend to a shallow level against conductive cooling to the seafloor. By contrast, with slow upwelling beneath slow-spreading ridges, conductive cooling to the seafloor extends to a great depth against the adiabat. Hence, the depth of P_F decreases, decompression interval ($P_O - P_F$) increases, and thus the extent of melting F ($\propto P_O-P_F$) increases with increasing spreading rate. A recent study using updated AP data further supports the finding by Niu and Hékinian (1997a) that the extent of ridge mantle melting increases with increasing spreading rate (Regelous et al., 2016).

3.3. The *lid-effect* on ridge mantle melting: Evidence from the correlation of MORB chemistry with ridge depth

While the ~ 60,000 km long global encircling ocean ridge system is considered to be the largest mountain ranges in ocean basins, the ridge depth varies significantly from near sea level around Iceland to up to 5500 m below sea level in the Cayman Trough. On average, the shallower ridge depth along the fast-spreading East Pacific Rise and the deeper ridge depth at many slow-spreading ridge segments suggest that ridge depth may increase with decreasing spreading rate, but this expected correlation is essentially absent with large amplitude of ridge depth variation towards slow-spreading ridges (Niu, 2016a). Hence, any correlation between spreading rate and ridge depth, if present, is insignificant. The large ridge depth variation must be isostatically compensated by the density variation of the underlying mantle material.

Therefore, alternative variables must be explored. Mantle temperature variation and compositional variation are possible causes because earth's surface elevation, including seafloor depth variation, must correlate with density structure of the subsurface (below seafloor) rocks as a function of temperature or composition. Except for ridges around Iceland where mantle temperature may be high, there is no evidence for large sub-ridge mantle temperature variation on a global scale, perhaps, no more than 50 K if any (Niu and O'Hara, 2006). The interpreted 250 K mantle temperature variation advocated by Langmuir's research team (see Fig. 6) does not exist because it is an artifact as the result of using MORB Fe_8 that is invalid and has no petrological significance (Niu and O'Hara, 2008; Niu, 2016a; also see above). These analyses leave fertile mantle compositional variation as the sole variable that controls the ocean ridge depth variation on a global scale.

The significant correlation of MORB major element compositions with ridge axial depth (Fig. 9a,b) is not a cause-and-effect relationship. Both are two different effects of a common cause. The common cause is the fertile mantle compositional variation, which is predicted to determine [1] variation in both composition and mode of mantle mineralogy, [2] variation of mantle density, [3] variation of ridge axial depth, [4] source inherited MORB compositional variation, [5] density-controlled variation in the maximum extent of mantle upwelling, [6] apparent variation in the extent of melting, and [7] the correlated variation of MORB chemistry with ridge axial depth as shown in Fig. 9c (also see Niu and O'Hara, 2008; Niu, 2016a).

Fig. 9c illustrates consistently the above predicted correlations. The mantle source is progressively more enriched (or less depleted) from beneath shallow ridges to beneath deep ridges, pointing to increasing modal garnet jadeite/diopside ratio in clinopyroxene, and pyroxenes/olivine ratio, thus a progressively denser mineral assemblage towards beneath deeper ridges. This explains straightforwardly why deep ridges underlain by fertile and denser asthenospheric mantle are deep and why shallow ridges underlain by depleted and less dense asthenosphere are shallow (see Niu and O'Hara, 2008). In addition, dense fertile mantle beneath deep ridges upwells reluctantly in response to plate separation, which leads to limited extent/amplitude of upwelling, allowing conductive cooling to penetrate to a great depth, making a thickened conductive thermal boundary layer (CTBL, region②), forcing melting to stop at a deep level (P_F), thus having a short melting interval (P_O-P_F), melting less, and producing probably a thin magmatic crust relative to the more refractory fertile mantle beneath shallow ridges. Therefore, the correlations in Fig. 9a,b also result from the *lid-effect*. Hence, the global MORB compositional systematics (Fig. 9b and c) are the net effect of [1] fertile mantle source inheritance and [2] varying extent of melting controlled by the varying amplitude of upwelling and decompression melting as the result of mantle density variations ultimately still controlled by fertile mantle compositional variation. The recent study by Dick and co-workers supports this understanding (Zhou and Dick, 2013; Dick and Zhou, 2015). Fertile mantle compositional control on mantle melting processes and MORB compositions have been reported in many regional and local studies (e.g., Schilling et al., 1983; Langmuir et al., 1986; Natland, 1989; Sinton et al., 1991; Perfit et al., 1994; Niu and Batiza, 1994; Castillo et al., 1998; Niu et al., 1999, 2001; Michael et al., 2003; Gill et al., 2016). It is particularly important to note that for a given ridge segment or fertile mantle domain, MORB derived from an isotopically and incompatible element enriched source have low FeO and CaO/Al_2O_3 (e.g., Batiza and Niu, 1992; Niu et al., 2002), which echoes the observations in Fig. 9a,b. Importantly, a recent near-ridge seamount MORB study shows significantly correlated variations of Fe isotope ratios with radiogenic isotopes and the abundances and ratios of incompatible elements (Sun et al, 2020a).

It is important to note that for a thermal expansion coefficient of $\alpha = 3 \times 10^{-5}$ K^{-1} for

mantle peridotites, the effect of temperature variation on mantle density is rather small compared to the effect of compositional variation. For example, mantle density decrease of ~ 1% for compositionally depleted mantle as a result of prior melt extraction would be equivalent to raising mantle temperature by 330 K (Niu and Batiza, 1991b; Niu et al., 2003; Niu and O'Hara, 2008). It is also worth to emphasize that it is straightforward that the enriched (or less depleted) mantle with higher Fe/Mg (e.g., Mg# = Mg/[Mg+Fe^{2+}] < 0.89) is readily understood to be denser than the depleted (or less enriched) mantle with slightly higher Mg/Fe (e.g., Mg# = Mg/[Mg+Fe^{2+}] > 0.90), but the effect of higher Al_2O_3 in the enriched (or less depleted) mantle is far more important because of the formation and stability of garnet, which has the greatest density of all the mantle minerals; 1.0 wt.% Al_2O_3 can make up to 5 wt.% garnet (see Niu et al., 2003; Niu and O'Hara, 2008) as illustrated in Fig. 9c.

To help readers better appreciate the geodynamic significance of compositional (vs. "thermal") buoyancy contrast, we can compare the largest topographic contrast on the Earth: the compositionally buoyant continental lithosphere (the crust and mantle lithosphere) and the compositionally dense oceanic lithosphere despite the fact that the oceanic lithosphere is "hotter" than continental lithosphere with mean per-square-meter heat flow ratio of 105.4/70.9 ≈ 1.49, which is also understood by the steeper geotherm beneath oceans (i.e., dT/dP$_{[Oceanic]}$ > dT/dP $_{[Continental]}$ (Davies and Davies, 2010; Niu et al., 2003; Niu, 2016a,b). Although the latter is related to the thin lithosphere beneath oceans than beneath continents, the fact that the thinned lithosphere (~ < 80 km) beneath eastern continental China since the Cenozoic (e.g., Guo et al., 2020; Sun et al., 2020b) is thinner than the mature seafloor lithosphere of ~ 90 km (e.g., Niu and Green, 2018), yet still sits above the sea level demonstrates the significance of compositional buoyancy variation that controls the earth's surface topography (both on land and beneath oceans). Similarly, the topographic contrast between the hilly lowland in eastern China (< ~ 200 m above sea level) and the high plateaus in western China (> 1500 m above sea level) further illustrates in simple clarity the subsurface compositional buoyancy contrasts that determines the surface elevation (see Section 6 below).

The *lid-effect* on mantle melting beneath *intra-plate ocean islands* for OIB

The recognition of the *lid effect* on ocean ridge mantle melting (Niu and Hékinian, 1997a; Niu and O'Hara, 2008), along with the work in the literature (Ellam, 1992; Haase, 1996), offers an imputes for further testing the hypothesis. We thus carried out a global analysis of OIB (Humphreys and Niu, 2009; Niu et al., 2011) because the thickness (*L*) of oceanic lithospheric lid varies significantly as a function of seafloor age (*t*), at least for seafloor younger than ~ 70 Ma, i.e., $L \propto t^{1/2}$ as the result of conductive heat loss to the seafloor and thermal contraction with time and because the thickness (*L*) or age (*t*) of the lithosphere at the time of OIB volcanism is known or can be well constrained (e.g., Parsons and Sclater, 1977; Parsons and McKenzie, 1978; Sclater et al., 1980; Stein and Stein, 1992; Niu and Green, 2018). Fig. 10a shows the correlated variations of average global OIB compositions with the lithosphere thickness at the time of OIB volcanism (Humphreys and Niu, 2009; Niu et al., 2011), which is wholly consistent with the *lid effect*, i.e., OIB erupted on thin oceanic lithosphere (T$_{OL}$) have a petrological signature of high extent of melting (high F $\propto$ P$_O$-P$_F$) and low pressure of melt equilibration (i.e., shallow P$_F$ melt extraction), whereas OIB erupted on thick T$_{OL}$ have the signature of low extent of melting (low F $\propto$ P$_O$-P$_F$) and high pressure of melt equilibration (i.e., deep P$_F$ melt extraction) as illustrated in Fig. 10b. The base of the lithospheric lid is conceptually the lithosphere-asthenosphere boundary (LAB; Fig. 3) in terms of mantle melting as it is the pargasite (amphibole) dehydration solidus (e.g., Green et al., 2010; Niu

and Green, 2018).

We must point out that intraplate OIB such as basalts erupted on Hawaiian Islands are widely interpreted as resulting from decompression melting of thermally buoyant upwelling mantle plumes. If this interpretation is correct, then the hot upwelling mantle would intersect the solidus at great depths (i.e., high P_O with high T_{MP}) and OIB from different mantle plumes with varying T_{MP} would begin to melt at varying depths (i.e., variably high P_O and high T_{MP}) (e.g., Putirka, 2005, 2008; Herzberg et al., 2007; Lee et al., 2009). However, the OIB data (Fig. 10a) do not show evidence for such varying P_O and thus T_{MP}, but varying P_F, the *lid effect* (Niu and Green, 2018). This is expected because erupted basalts do not have the memory of initial depth of melting as the result of effective and efficient melt-solid equilibration during decompression melting as illustrated in Fig. 5 (see Section 2.4). The $[Sm/Yb]_N$ ratio is often used to infer depth of mantle melting with low values as indicating shallow melting in the spinel peridotite stability field (i.e., the mineralogy of olivine [ol]+ orthopyroxene [opx] + clinopyroxene [cpx] + spinel) and high values as indicating deep melting with garnet as a residual phase in the garnet peridotite stability field (i.e., the mineralogy of ol + opx + cpx + garnet [gnt]). This is because among all the mantle minerals, garnet is the only phase with strong preference to hold Yb over Sm (e.g., $Kd_{[Yb/Sm]\text{-gnt}} \approx 32 \gg Kd_{[Yb/Sm]\text{-cpx}} \approx 1.3$; see compilation in Niu et al., 1996), giving rise to low Yb and thus high Sm/Yb in the melt, which is called the *garnet signature*. However, the data in Fig. 10a indicate that mantle melting for all the OIB begins in the garnet peridotite stability field and the decreasing $[Sm/Yb]_N$ with decreasing T_{OL} ($\propto$ LAB depth) results from continued decompression melting in the spinel peridotite stability field, which progressively dilutes the garnet signature. Therefore, all the intraplate melting for OIB begins deep in the garnet peridotite stability, but the data do not have the memory of P_O variation between OIB suites even if T_{MP} may indeed vary between intraplate ocean islands and island groups.

Therefore, like MORB, OIB do not preserve the information on initial depth of mantle melting and thermobarometers built on olivine phenocrysts and basalts, albeit useful (Putirka, 2005, 2008; Herzberg et al., 2007; Lee et al., 2009), provide no information on T_{MP} (see Section 2.4).

The *lid-effect* on mantle wedge melting above subduction zones for VAB: A new and consistent perspective

I use the phrase "a new and consistent perspective" to inform the community that the apparently complex subduction-zone magmatism may in fact be much simpler thanks to the data compilation by Turner and Langmuir (2015a,b) although my understanding of the data differs from theirs.

Volcanic arc basalts (VAB) are widely accepted as resulting from slab dehydration induced mantle wedge melting. This is also called flux melting because the melting is triggered by influx of water-dominated fluids from the subducting slab, which lowers the mantle wedge solidus and makes melting possible (Fig. 3e,d). This interpretation is reasonable because VAB have distinct compositions enriched in water and water-soluble elements (e.g., U, K, Sr, Pb) but depleted in water-insoluble elements (e.g., Ti, Nb, Ta) (e.g., Tatsumi and Eggins, 1995). However, whether the extent of mantle melting may vary between VAB systems is unclear, and if it does, what may actually control the extent of melting is also unclear. By emphasizing water-facilitated melting, it is expected that the extent of mantle wedge melting must be higher than sub-ridge mantle melting for MORB because of significantly lowered wet solidus (e.g., Stolper and Newman, 1993), but the extent of melting is also expected to be constrained by the lithospheric *lid* as discussed above (Figs. 3, 8-10). Indeed, Plank and Langmuir (1988) analyzed the then available global VAB data and show the presence of correlated variations of

arc-averaged VAB major element compositions with arc crustal thickness, i.e., $Na_{6.0}$ (Na_2O corrected to MgO = 6.0 wt.%) increases whereas $Ca_{6.0}$ (CaO corrected to MgO = 6.0 wt.%) decreases with increasing crustal thickness. The authors interpreted these correlations as resulting from varying extent of melting; thick crust limits melting to a deep depth, giving a VAB petrological signature of low extent of melting (high $Na_{6.0}$ and low $Ca_{6.0}$), whereas thin crust allows melting to stop at a shallow depth, giving a VAB signature of high extent of melting (low $Na_{6.0}$ and high $Ca_{6.0}$). Using the updated global data, Turner and Langmuir (2015a,b) confirmed the same observations using more chemical parameters consistent with varying extent of melting (see Fig. 11a), which is apparently consistent with the *lid effect* although a paradoxical issue must be addressed (see below).

These authors choose to interpret the VAB systematics (Fig. 11a) as controlled by mantle wedge temperature variation as advocated in recent studies (e.g., England et al., 2004; England and Katz, 2010). Following their study of the Chilean Southern volcanic zone VAB (Turner et al., 2016), Turner and Langmuir (2015a.b) interpret the global VAB systematics (Fig. 11a) as resulting from mantle wedge temperature structure variation as illustrated in Fig. 11b-d, i.e., the mantle wedge is up to 250 K hotter beneath thin lithosphere than beneath thick lithosphere with respect to the dry solidus. Hence, the hot mantle wedge beneath thin lithosphere melts more than the cold mantle wedge beneath thick lithosphere. This apparently reasonable interpretation is in fact conceptually misguiding because the interpreted mantle wedge temperature structure has nothing to do with mantle wedge asthenosphere where melting takes place and whose temperature is controlled by T_{MP} of the convective mantle wedge asthenosphere and the subducting slab which drives mantle wedge convection while also serving as a heat sink. Objectively and rigorously, the VAB systematics (Fig. 11a) is not caused by mantle wedge temperature variation but is a straightforward consequence of the *lid effect*, which requires that decompression melting be the dominant mode of mantle wedge melting in addition to flux-melting for the onset of melting. This can be elucidated below with conceptual clarifications and caveats.

5.1. The nature of the lithospheric lid overlying the mantle wedge

From the observation (Fig. 11a) to the interpretation (Fig. 11b-c) is the hidden assumption that the arc crust and lithosphere are "equivalent", which cannot be true unless the crust is in direct contact with the asthenosphere without a lithospheric mantle root. The latter cannot be true without fast lithospheric extension and rifting, which is not the case beneath modern volcanic arcs above subduction zones. The fact that a number of VAB suites contain mantle peridotite xenoliths (e.g., Parkinson and Arculus, 1999; Ionov et al., 2012; Tollan et al., 2015) manifests the presence of mantle lithosphere beneath arc crust. The process of mantle xenolith inclusion can be explained using understood mechanism of mantle xenolith incorporation in some OIB and continental alkali basalts with abundant volatiles. Primitive VAB melts formed in the asthenospheric mantle wedge contain abundant dissolved water, whose exsolution during ascent due to decompression (reduced solubility in the melt; Sparks et al., 2000; Cashman and Blundy, 2000; Blundy and Cashman, 2005) results in volume expansion and elevated viscosity to develop destructive power to incorporate the conduit walls of the lithospheric mantle as xenoliths carried to the surface during VAB eruption (see Sun et al., 2017, 2020b for mechanism). Hence, it is the thickness of the entire lithosphere, i.e., the LAB depth, that caps the mantle wedge melting not the crust (Fig. 11b,c). In this case, the correlation of VAB geochemistry with crustal thickness (Moho depth) may mean the correlation with the LAB depth, i.e., the arc crustal thickness is proportional to the lithosphere thickness (i.e., Moho depth ∝ LAB depth). This is possible because continental arc with thicker continental crust (purple solid circles in Fig. 11a) is expected to have a thicker

lithospheric mantle root whereas thinner oceanic arc crust (blue solid circles in Fig. 11a) is expected to have a thinner lithospheric mantle root. This is likely to be true in general inferred from global surface elevation and isostasy, but it is imperative to acquire high resolution seismic data on both LAB and Moho depths to verify this hypothesis in the future.

5.2. The nature of volcanic arc crust

We should note the contrast between the ocean crust and arc crust. The ocean crust, with a few localized exceptions at some slow-spreading ridges (Niu, 1997), is solidified magmas formed at ocean ridges. The observation (Fig. 11a) says that the thicker arc crust is, the lesser of which is of arc magmatic origin as a result of mantle wedge melting. This inverse correlation of the extent of mantle melting with arc crustal thickness contradicts the belief that arc crust is magmatic construct. This contradiction reflects widespread misconceptions because much of the arc crust must be pre-arc crustal basement of long and complex histories already in place at the time of subduction initiation (Niu et al., 2003; Niu, 2016b). One may argue that thicker arc crust may mean longer arc volcanism in one place for tens of millions of years or that the initial arc crust was exceptionally voluminous. However, there is no evidence to support such arguments. For example, there is no evidence that the thicker arc crust (~ 35 km) above the continental basement of the Japanese arcs records longer volcanic history than the thinner arc crust (~ 17-20 km) above the "oceanic" basement of Tonga and Mariana arcs with similar timing of subduction initiation at ~ 52 Ma (Stern, 2002). The young Ryuku arc (< 12 Ma) above the continental basement (Chinese continental shelf) has a thick crust (~ 25 km) with no evidence of exceptionally voluminous magmatism. Hence, this observation and conceptual understanding here are of far-reaching significance for models of subduction initiation (Niu et al., 2003; Niu, 2014) and for reevaluating the widely accepted "island-arc model" for continental crust accretion (see Niu et al., 2013).

5.3. What controls mantle wedge thermal structure?

Turner and Langmuir (2015a,b) implicitly assume that the lithosphere thickness (inferred from crustal thickness, i.e., LAB depth $\propto$ Moho depth) controls mantle wedge temperature structure (Fig. 11b-d) and ascribe the extent of mantle wedge melting inferred from the VAB compositions (Fig. 11a) as resulting from mantle wedge temperature structure control with temperature variation of up to 250 K (Fig. 11d). This nested interpretation is confusing and is erroneous in both concept and practice. The LAB is likely the amphibole (pargasite) dehydration solidus, which is an isotherm of ~ 1100°C at all pressures $\leq$ 3 GPa (Niu and Green, 2018). So, the conductive geotherm of the thin lithosphere ($dT/dP_{[LITH\ THIN]}$) is steeper than that of the thick lithosphere ($dT/dP_{[LITH\ THICK]}$) (Fig. 11e), making the convective asthenosphere pushed down at greater depth beneath thick lithosphere than beneath thin lithosphere. The thickness of the *conductive* lithosphere is irrelevant to, and thus cannot be used to measure, the temperature of the underlain *convective* asthenosphere. If we followed the logic in Fig. 11b-d, we would say that the mantle beneath ocean ridges with thin lithosphere must be hotter than the mantle beneath Hawaiian Islands with thick lithosphere, which is simply wrong. The concept of T_{MP} was introduced (McKenzie and Bickle, 1988) to discuss lateral mantle temperature variation of convective asthenosphere at similar depth with $dT/dP_{[Adiabat]}$, which is irrelevant to $dT/dP_{[Conductive]}$ of lithospheric lid.

The logical discussion on mantle wedge temperature must be based on initial depth of melting, which remains debated, but must take place right below active arc volcanoes some distance above the slab surface controlled by the interplay of [1] slab-derived fluids, [2] T_{MP} and [3] effect of the subducting slab (Gill, 1981; Arculus, 1994; Tatsumi and Eggins, 1995;

Stern, 2002; Elliott, 2003; England et al., 2004; Syracuse and Abers, 2006; Syracuse et al., 2010; England and Katz, 2010; Grove et al., 2012).

[1] The effect of slab-derived fluids is understood to develop water-saturated wet solidus that triggers mantle wedge melting, which is deep in the asthenosphere and *does not know* the thickness of the overlain lithospheric lid.

[2] The role of T_{MP} maintained by the convective asthenosphere with $dT/dP_{[Adiabat]}$ is necessarily important and is unaffected by the lithospheric lid above with $dT/dP_{[Conductive]}$ and the cold subducting slab below.

[3] The effect of the subducting slab is often described by a slab thermal parameter (Φ = plate age * vertical descent rate; Syracuse et al., 2010). The greater the Φ value is, the more cold-slab mass is subducted per unit time and thus serves as a heat sink to cool the mantle wedge.

However, it is the subducting slab that drives mantle wedge convection that maintains the hot mantle wedge with $dT/dP_{[Adiabat]}$, otherwise the mantle wedge would freeze. The fast descent of the slab will induce fast lateral hot/warm asthenospheric material supply towards the slab (i.e., the corner flow; England et al., 2004), so [3] cools the mantle wedge while also inducing heat supply to maintain [2]. Thus, the thermal effects of [2] and [3] may be largely canceled out, depending on the depth and extent of slab-wedge decoupling (e.g., Wada et al., 2008; Syracuse et al., 2010). Nevertheless, the combined net thermal effect of [2] and [3] could still play some role (England and Katz, 2010), but this is unlikely to be important for arc magmatism because the observations (Fig. 11a) do not record such combined thermal effect.

Turner et al. (2016) show that the estimated extent of melting varies along the Chilean South Volcanic Zone (~ 33° - 43°S) as a function of the Moho depth with a constant thermal parameter (i.e., $\Delta\Phi \approx 0$), which denies the effect of slab cooling, but supports the *lid effect* on the VAB magmatism. Turner and Langmuir (2016b) argue, however, with confusing inference that the difference between observed $Na_{6.0}$ and $Na_{6.0}$ predicted from regression against crustal thickness (Fig. 11a) correlates with a composite parameter $V\sin(\theta)$ (subducting slab speed [V] and slab dip angle [θ]) and interpret this correlation as slab cooling effect on mantle wedge temperature. The slab with smaller dip angle is interpreted to cool mantle wedge more with lower extent of melting. This interpretation contradicts that of Turner et al. (2016) and is physically incorrect because mathematically $V\sin(\theta)$ is proportional to the depth of the slab surface beneath arc volcanoes. For example, for a given LAB depth (i.e., P_F), the extent of decompression melting $F \propto P_O-P_F$ decreases with decreasing $\sin(\theta)$ and θ (Fig. 11e,f). This is conceptually the same as the *lid effect*, not thermal effect (see below).

5.4. Diapiric upwelling, decompression melting and lid effect on the extent of melting and VAB compositions

The observations (Fig. 11a) demonstrate that it is the lithosphere thickness variation that controls the extent of mantle wedge melting and the global VAB compositions as illustrated schematically for scenarios of thin (*e*) and thick (*f*) lithosphere with $dT/dP_{[THIN]} > dT/dP_{[THICK]}$ and $LAB_{[THIN]} < LAB_{[THICK]}$. Mantle wedge melting begins at Po and the melting mantle will rise because of buoyancy, and the rising melting mantle continues to melt progressively more by decompression until capped by the lithospheric lid at the LAB. As expected, VAB erupted on thick lithosphere have the signature of low extent of melting (Fig. 11a) because of short decompression melting interval $[P_O–P_F]_{THICK}$ whereas VAB erupted on thin lithosphere have the signature of high extent of melting (Fig. 11a) because of taller decompression melting interval $[P_O–P_F]_{THIN}$. We should note that at ocean ridges, decompression melting results from plate separation induced passive mantle upwelling and decompression melting, but there is no

obvious mechanism for mantle wedge upwelling. Fig. 11e,f shows schematically that the upwelling results from initial melting that develops into growing and buoyant diapirs (e.g., Green and Ringwood, 1967; Wyllie, 1971) driven by the Stakes-law for continued decompression melting. That is, mantle wedge melting results from [1] slab fluid caused wet solidus; [2] initial flux melting facilitates the development of growing and ascending diapirs; [3] diapiric upwelling and decompression melting; [4] decompression melting cessation capped at the LAB, the base of the conductive lithospheric lid. Hence, lithospheric thickness variation, the *lid effect*, exerts the primary control on the extent of mantle wedge melting and VAB composition (Fig. 11a). The combined net thermal effect of T_{MP} and slab cooling, which must play a role, is not recorded in the VAB petrology and geochemistry. It is possible and likely also that the combined thermal effect on VAB composition may have been obliterated by the effective and efficient melt-solid equilibration in the rising melting mantle diapirs as in the case of MORB and OIB. That is, VAB have no memory of P_O (Figs. 5, 8-10).

5.5. VAB preserves the garnet signature

We note from Fig. 11a that the VAB preserve the garnet signature whose intensity (high Dy/Yb and low Sc) decreases with increasing extent of melting from beneath thick lithosphere (less dilution) to beneath thin lithosphere (more dilution). One may interpret the varying Sc and Dy/Yb as the signature clinopyroxene, but this is a clear garnet signature because $Kd_{[Yb/Dy]-cpx} \approx 1 < Kd_{[Yb/Dy]-gnt} \approx 3.5$ and $Kd_{Sc-cpx} \approx 3 < Kd_{Sc-gnt} \approx 4$ (see Niu et al., 1996), indicating that clinopyroxene will not cause Dy/Yb variation, but garnet does. This recognition offers important insights: [1] mantle wedge melting do start in the garnet peridotite stability field with garnet as a residual phase, and the garnet signature is progressively more diluted with increasing extent of diapiric decompression melting in the spinel peridotite stability field beneath thin lithosphere as seen in OIB (Fig. 10); [2] it is also probable that eclogite in the subducting ocean crust may participate in and contribute to mantle wedge melting most likely at the onset of melting at P_O, which requires further investigation.

The *lid-effect* on mantle melting beneath continents and CIB

Cenozoic basalt volcanism in continental interiors occurs where lithosphere is thin or recently thinned caused by water introduction through seafloor subduction currently or in no distant past such as eastern China, eastern Australia, western Mediterranean and western USA (Niu, 2006, 2014). Eastern China is a type region for studying intra-continental mantle melting because it has a history of widespread lithosphere thinning in the Mesozoic by means of basal hydration weakening associated with Paleo-Pacific plate subduction (see Niu, 2005a, 2014, Niu et al., 2015), which developed oceanic type seismic low velocity zone (LVZ) beneath the region (Niu, 2014) that is well maintained in the Cenozoic by dehydration of the present-day Pacific plate stagnant in the mantle transition zone (Karason and van der Hilst, 2000; Niu, 2014). The widespread Cenozoic basalt volcanism in eastern China is the consequence of this LVZ (Figs. 12-13).

Fig. 12 summarizes the topography of continental China and the adjacent regions and the interpreted basaltic magmatism in eastern China in the context of plate tectonics. The great gradient line (GGL; white dashed line) marks the contrast in elevation, gravity anomaly, crustal thickness and mantle seismic velocity from high plateaus in the west to hilly low plains of eastern China, which manifests varying lithosphere thickness from ≥150 km beneath the plateaus in the west to ≤ 80 km beneath eastern China (Niu 2005a). The three Cenozoic lava fields across the GGL (rectangle with arrowed traverse A in Fig. 12a) show

compositional systematics that are a straightforward consequence of the *lid effect* as illustrated in Fig. 13a. In a spatial stretch of ~ 250 km from southeast to northwest across the GGL, the elevation increases from ~ 600 m to ~ 1400 m above sea level, corresponding to lithosphere thickness (the LAB depth) increase from ~ 80 km to ~ 120 km (Guo et al., 2020), the basalts are characterized by decreasing extent of melting (i.e., increasing Ti_{72}, P_{72}, K_{72}, $[La/Sm]_N$ and $[Sm/Yb]_N$) and increasing pressure (i.e., LAB depth) of melt extraction (i.e., decreasing Si_{72} and increasing Mg_{72}, Fe_{72}, $[Sm/Yb]_N$).

Furthermore, all the Cenozoic alkali basalts in eastern China carry abundant mantle xenoliths, and ten suites of these basalts distributed over a north-south stretch in excess of 2,500 km contain high pressure clinopyroxene megacrysts (tall triangles in Fig. 12a; Fig. 13b). The calculated crystallization pressure of the megacrysts, fully consistent with crystallization from a "stable magma reservoir" close beneath the LAB, correlates well with the geochemistry of the host basalts. These correlated variations are manifestations of the *lid effect*, i.e., with increasing pressure of clinopyroxene megacryst crystallization (i.e., the LAB depth), the compositions of the melt indicate increasing pressure of melt extraction (decreasing Si_{72} and Al_{72}, and increasing Fe_{72}, Mg_{72} and $[Sm/Yb]_N$) and decreasing extent of melting (increasing Ti_{72}, P_{72}, $[Sm/Yb]_N$). The strength of the garnet signature, as predicted, increases with increasing pressure (increasing $[Sm/Yb]_N$ and decreasing Sc) because Sc and Yb are highly compatible in garnet (Sun et al., 2020b).

The *lid-effect* on mantle melting for large igneous provinces (LIPs) on land and in ocean basins

Many intra-plate basaltic volcanoes away from plate boundaries have been interpreted as resulting from decompression melting of dynamically upwelling hot mantle plumes originated from the hot thermal boundary layer in the D" region at the core-mantle boundary (e.g., Morgan, 1971; Campbell and Griffiths, 1990; Griffiths and Campbell, 1009; Duncan and Richards, 1991; Sleep, 1990, 1992; Coffin and Eldholm, 1994; Davies, 1999). But such lower-to-upper mantle material transfer cannot happen without a plume head with sufficient buoyancy (Hill et al., 1992; Campbell and Griffiths, 1990; Duncan and Richards, 1991; Davies and Richards, 1992; Davies, 2005; Niu et al., 2017). Decompression melting of plume heads produces large igneous provinces (LIPs) with large basalt volumes emplaced in short time periods, forming oceanic plateaus in ocean basins (e.g., Ontong Java Plateau in the Pacific and Kerguelen Plateau in the Indian Ocean) and continental flood basalt provides (e.g., Siberian Trap, Deccan Trap, Columbia River Basalt) (Fig. 14a,b). Following the emplacement of LIPs are long-lived volcanic activities that may produce volcanic chains (or hotspot tracks) such as age-progression seamount chains in ocean basins if the plates move fast relative to the volcanic centers. The most significant in this context concerns the question whether mantle plume heads can cause continental breakup, especially breakup and dispersal of supercontinents because there has been voluminous literature in recent decades that correlates continental breakup in time and space with mantle plumes (Richards et al., 1989; Hill, 1991; Hill et al., 1992; Storey, 1995; Li et al., 1999, 2003; Condie, 2004; Zhong et al., 2007; Buiter and Torsvik, 2014; Zhang et al., 2018). I have recently demonstrated that continental breakup is a straightforward consequence of plate tectonics without requiring mantle plumes, and mantle plumes, if needed, may be of help at early rifting stage, but cannot lead to complete breakup, let alone to drive long distance dispersal of broken continents (Niu, 2020a). From the perspective of scientific developments, I predict that many advocates will continue to disagree on my objective, logical and rigorous analysis. So, it is necessary and particularly pertinent here to discuss the issue in the context of the *lid effect* on mantle melting and global basalt magmatism.

Fig. 14c shows in P-T space the mantle solidus (McKenzie and Bickle, 1988) and adiabat for two scenarios with T_{MP} = 1600°C for mantle plumes of dynamic upwelling and T_{MP} = 1350°C appropriate for passive upwelling beneath ocean ridges for comparison. To illustrate the concept, we can choose T_{MP} = 1600°C for the plume scenario, which is likely hotter than widely assumed. P_O is the depth of rising mantle plume that intersects the solidus and begins to melt. For comparison, we also show the depth of P_O for cooler mantle with T_{MP} = 1550°C and 1500°C. Fig. 14d shows three scenarios of varying thickness of continental lithosphere when impacted by a rising mantle plume head (after Niu, 2020a). The key concepts and logical reasoning are given below:

[1] The adiabatically rising mantle plume head begins to melt when intersecting the solidus at P_O ≈ 140 km.

[2] The rising mantle plume head continues to melt until capped by the lithosphere at P_F, ~ 120 km, which is the LAB, equivalent to average continental lithosphere thickness.

[3] Melting cannot happen in the lithosphere as it is under sub-solidus conditions (except for volumetrically small metasomatic veins or veinlets of lower solidus temperature).

[4] A spherical plume head 1000 km across (R = 500 km) that flattens to a disk 2000 km across (r = 1000 km) when reaching the lithosphere (see Fig. 14a,b; Campbell, 2007) will have thickness of ~ 167 km.

[5] To be conservative, we assume the flattened lithosphere to be about half of the thickness ~ 84 km.

[6] Whether melting actually occurs or not and if so to what extent, strictly depends on the lithospheric thickness (see above; Niu et al., 2011) as quantified (Watson and McKenzie, 1991; White and McKenzie, 1995).

[7] No matter how hot the mantle plume head may be, melting cannot happen beneath thickened lithosphere such as [II] and [III] but can take place beneath thin lithosphere such as [I].

[8] The extent of melting beneath the thin lithosphere (scenario [I]) is likely very low (no more than ~ 5%; Watson and McKenzie, 1991; White and McKenzie, 1995), and with H_2O-dominated volatiles entering the melt, the viscosity of the residual plume head would be highly elevated (e.g., from ~ 10^{19} to ~ 10^{21} Pa s; e.g., Hirth and Kohlstedt 1996; Karato 2003). The plume head would be too viscous to flow, thus contributing to the new accretion of the lithosphere, which thickens (*not* thins) the lithosphere from the prior ~ 120 km to ~ 200 km.

This simple analysis, despite the uncertainties, is informative and states that the effect of plume head arrival will make the lithosphere thicker, not thinner, against common perception, let alone to cause lithosphere breakup (vs. scenario in Fig. 14b). We can predict that the arrival of plume heads may in fact facilitate consolidating and stabilizing continental lithosphere to contribute to cratonization over earth's history.

Because melting cannot take place beneath thickened lithosphere under sub-solidus conditions (e.g., [II] and [III]), the physical effect of plume heads on the existing lithosphere is limited, thus unlikely causing lithosphere breakup (vs. scenario in Fig. 14b). Because of the hot plume head, minute H_2O-CO_2-rich low-degree (~ 1 % or lower) melt may be produced to migrate and metasomatize the overlying lithosphere but is inadequate to produce LIPs.

[9] Lithosphere uplift or doming (scenario in Fig. 14b) can take place, but this will not change the LAB depth without surface erosion (or exhumation). A maximum uplift and erosion of 600 m is rather small and even 2000 m is still too small to affect the LAB at great depths (~ 120 km, ~ 150 km, and ~ 200 km scenarios [I], [II] and [III]). Hence, mantle plume heads would have very limited impact on the mature and thickened lithosphere without melting but can have large impact on thin or thinned

lithosphere by melting with the extent of impact increasing with decreasing lithosphere thickness. This suggests that the mantle plume head effect is best observed beneath thin or thinned lithosphere such as beneath prior between-craton sutures, especially extensional settings like continental rifts and spreading centers in ocean basins (Niu and Hékinian, 2004; Niu, 2020a).

We thus cannot avoid the conclusions: [1] mantle plumes, no matter how hot and how big a plume head may be, cannot melt by decompression to produce LIPs beneath thickened cratonic lithospheric *lid*; [2] continental rifting and breakup cannot take place within thickened and physically coherent cratons by mantle plumes, but must take place along prior zones of weakness such as sutures (McKenzie et al., 2015; Niu, 2020); [3] cratonic lithosphere can be thinned and destroyed through basal hydration weakening as was the case in eastern continental China in the Mesozoic (Niu, 2005a, 2014); [4] LIPs in the geological record indicate thin lithosphere at the time of volcanism; [5] it follows that if there are/were many more mantle plumes and plume heads beneath continents at present and probably also in Earth's history, only those arriving beneath thin or thinned lithosphere could be recognized through LIPs (Davies et al., 2015); [6] Hence, it is the size, thickness and strength of the continental lithosphere that determines whether a mantle plume can surface and whether a mantle plume can break up the continents, not the other way around; [7] Arrival of mantle plume heads beneath coherent continental lithosphere may in fact facilitate cratonization.

Hence, lithosphere thickness has profound and deterministic control on sublithospheric mantle melting and basaltic magmatism on local, regional and global scales.

Summary

The idea that *mantle (potential) temperature (T_{MP}) variation controls the extent of mantle melting and basalt composition* (i.e., "temperature control") developed in 1980s has since become the *paradigm* on basalt petrogenesis. My research over the past 30 years on the subject demonstrates repeatedly that this paradigm is unsupported by observations and needs change. With the principle that large scale Earth processes are likely very simple, but the key skill to discover the simplicity is to correctly identify the primary variables that control the processes (Niu, 2020b), I devoted effort on global observations to seek key variables controlling mantle melting which leads to the conclusion that lithosphere thickness variation (i.e., the *lid effect*) exerts the primary control on the extent of mantle melting, depth/pressure of melt extraction and basalt compositions in *all tectonic settings* on Earth: mid-ocean ridge basalts (MORB), intra-plate ocean island basalts (OIB), volcanic arc basalts above subduction zones (VAB) and basalts in continental interiors (CIB). Below are condensed summary of rigorous analyses, key observations, and future work.

(1) The common perception that solid rock melting needs heating gives the impression of temperature control and thus the popular acceptance of the paradigm. But the understood mantle melting mechanisms (Fig. 3) do not require excess heat or temperature but require conditions that place the asthenospheric mantle onto or above the solidus (dry or wet solidus) in P-T space although the initial depth of melting (P_O) may vary.

(2) The extent of mantle melting (F) is not controlled by P_O, but controlled by decompression interval P_O-P_F. That is. the final depth of decompression melting P_F at the LAB is important as it is the base of the conductive thermal boundary layer (CTBL) that varies between tectonic settings and can also vary vastly on all scales for a given tectonic setting, depending on the geological history.

(3) The effect of P_F on the extent of melting $F \propto P_O\text{-}P_F$ can be readily understood by comparing the scenarios of Iceland and Hawaii that are considered as two type hot mantle plumes with similarly hot and deep P_O, but hugely different P_F[Hawaii] $\approx$ 90 km > P_F [Iceland] < 20 km. If $P_O \approx$ 100 km, then the decompression melting interval would be $P_O\text{-}P_F$[Iceland] $\approx$ 80 km > $P_O\text{-}P_F$[Hawaii] $\approx$ 10 km. Hence, the extent of melting beneath the thin lithosphere in Iceland can be up to 8 times greater than that beneath the thick lithosphere in Hawaii (linear scaling is assumed here for conceptual clarity), which is consistent with their petrological and geochemical contrast (see discussion given in Niu et al., 2011). Therefore, lithosphere thickness variation, i.e., the lithospheric *lid effect*, is predicted to be the primary variable that controls the extent of mantle melting, pressure/depth of melt extraction at the LAB, and basalt compositions.

(4) Basalt compositions are known to vary as a function of fertile mantle composition, extent and pressure of melting and crustal level magma evolution. Once the effects of crustal level processes can be corrected for (largely removed), the data can be used to discuss mantle sources and processes. The significantly correlated variations of OIB compositions with the thickness of oceanic lithosphere at the time of volcanism (Fig. 10a) is the simple manifestation of the *lid effect* with OIB erupted on thick lithosphere having the petrological signature of low extent (low $F \propto P_O\text{-}P_F$) of melting and high pressure (high P_F = deep LAB) of melt extraction, whereas the opposite is true for OIB erupted on thin lithosphere (Fig. 10b). The same is true for CIB as demonstrated in Figs. 12-13. We should note that the compositional scatter about the systematic trends must be combined effect of mantle source compositional variation, initial depth (P_O) of melting due to T_{MP} variation or source fertility variation, and errors associated with fractionation correction. We *do not at all ignore all these factors*, but they are secondary and insignificant because they are overshadowed by the *lid effect*.

(5) The observations and analysis in (4) inform us explicitly that OIB and CIB do not record information on P_O, but well preserve the information on P_F at the LAB, the depth of melt extraction, which is the final depth of melting and melt-solid equilibration. Specifically, the pressure sensitive chemical parameters (i.e., $P_F \propto$ MgO, FeO, 1/SiO_2 and 1/Al_2O_3 [weakly]; Fig. 4) are well preserved to consistently record final depth of melt-solid equilibration beneath ocean basins (OIB; Fig. 10) and continental interiors (CIB; Fig. 13). These systematics are in fact predicted in terms of experimental petrology and effective melt-solid equilibration in the rising melting mantle (Fig. 5; Niu, 1997, 2016a).

(6) MORB compositional systematics as a function of ridge spreading rate variation (Fig. 8a) is a straightforward consequence of the *lid effect* (Figs. 8,9). Plate separation causes the sub-ridge mantle to rise and melt by decompression. Fast upwelling beneath fast-spreading ridges allows the adiabat to extend to a shallow level against conductive cooling to the seafloor, resulting in a thin CTBL, a great decompression interval ($P_O\text{-}P_{F, shallow}$) and high extent of melting. By contrast, slow upwelling beneath slow-spreading ridges allows conductive cooling to penetrate to a great depth against the adiabat, resulting in a thick CTBL, a small decompression interval ($P_O\text{-}P_{F, deep}$) and low extent of melting (Fig. 8a).

(7) MORB compositional systematics as a function of ridge axial depth variation (Fig. 9a) is also a consequence of the *lid effect* (Figs. 8,9). These correlated variations are very informative that fertile mantle source compositional variation plays a dynamic role (Niu et al., 2001; Niu and O'Hara, 2008). The ridge depth variation is the manifestation of sub-ridge mantle density variation because of major element compositional variation, from compositionally depleted and physically buoyant mantle beneath shallow ridges to

less depleted (or enriched) and denser mantle beneath deep ridges. Dense fertile mantle beneath deep ridges upwells reluctantly in response to plate separation, which leads to limited extent/amplitude of upwelling, allowing conductive cooling to penetrate to a great depth (P_F), shortening melting interval (P_O-P_F) and melting less relative to the more refractory and buoyant fertile mantle beneath shallow ridges (Fig. 9b). MORB compositional variations in Fig. 9a are consequence of the *lid effect* and the source compositional inheritance, both working in the same way.

(8) It is important to note that different from OIB and CIB, the *lid effect* on MORB petrogenesis is conspicuous in controlling the extent of melting as a function of spreading rate (Fig. 8) and ridge axial depth (Fig. 9), but no detectable pressure signature on P_F. This is expected because [1] the P_F depth (or thickness of the CTBL) variation along ocean ridges is small (compared to the scenarios of OIB and CIB), and [2] importantly the advanced MORB melting residues in the CTBL (Figs. 5,8a,9a), sampled as abyssal peridotites, are not simple residues, but have excess olivines crystallized from the ascending melts, pointing to effective olivine ($[Mg,Fe]_2SiO_4$) controlled melt-solid equilibration during ascent at varying depths shallower than P_F (Niu, 1997, 2004; Niu et al., 1997).

(9) While slab-dehydration induced mantle wedge melting or flux melting is the understood major mechanism of magma generation above subduction zones, the global VAB compositional systematics reported by Turner and Langmuir (2015a,b) is a straightforward consequence of the *lid effect*. Although these authors presented the correlations with arc crustal thickness (i.e., Moho depth vs. LAB), it is predicted that Moho depth $\propto$ LAB depth and more effort is needed to obtain high quality seismic data to resolve LAB depths beneath global volcanic arcs to further quantify the Moho $\propto$ LAB depth relationship. Note that Turner and Langmuir (2015a,b) incorrectly interpret the *lid effect* as mantle wedge temperature structure control by advocating hot mantle beneath thin arc lithosphere and cool mantle beneath thick arc lithosphere, which is the same as arguing for hot mantle beneath ocean ridges with thin lithosphere and cool mantle beneath ocean islands like Hawaii with think lithosphere.

(10) The observations that erupted basalts record P_F (i.e., the LAB depth), not P_O, in all settings (MORB, OIB, VAB and CIB) reiterate the fundamental understanding of effective melt-solid equilibration in the melting mantle (Fig. 5; Niu, 1997, 2016a). This is smoking-gun evidence that erupted basalts have no memory of initial depth of melting at least in terms of olivine-making elements Si, Mg and Fe. It follows in simple clarity that basalt olivine-based thermobarometers provide no information on P_O and T_{MP}. In other words, the calculated P_O and T_{MP} using such thermobarometers have no significance *unless* the lid effect is properly corrected for if possible (Niu et al., 2011). This new understanding requires thorough reevaluation of many discussions on P_O and T_{MP} in the literature.

(11) Mantle plumes or plume heads, no matter how big and how hot, will not melt beneath thickened *cratonic lithosphere lid*, which is below the solidus, will not surface and will not cause continental breakup. If anything, the arrival of mantle plumes and plume heads will contribute to new accretion of the lithosphere thickening, and importantly may facilitate stabilization of cratons, rather than causing continental breakup as popularly believed (Fig. 14; see Niu, 2020). Therefore, LIPs as a result of mantle plume head decompression melting must indicate the thin or thinned lithosphere at the time of LIP volcanism.

(12) Following all the above, we can add here that komatiite as a result of very high extent of mantle melting (high F $\propto$ P_O - P_F) requires not only deep initial melting (high P_O) but also shallow melting cessation (low P_F) under thin or very thin *lithospheric lid* although

Archean komatiites are often preserved in association with cratonic shields of thick lithosphere. This inference offers an additional perspective on understanding the petrogenesis of yet mysterious komatiites (see McKenzie, 2020).

(13) It may be too big wording to say *paradigm shift*, but the "temperature control" paradigm on basalt petrogenesis that is inconsistent with all the observations needs change in order to promote scientific progress forward. As the change from "temperature control" to "lid effect" is fundamental and may be unaccustomed to many, it will take time to convince the community through further debate. I endeavor to actively participate in this debate through this publication and future communications. To facilitate such debate, I offer the following two statements.

(14) [1] Global MORB (Figs. 8,9), OIB (Fig. 10), VAB (Figs. 11) and CIB (Fig. 13) compositions all show the *lid effect*, but do not show the effect of "temperature control" (i.e., P_O or T_{MP}), which may not be important at all in reality or, if any, may have been obliterated because of effective and efficient melt-solid equilibration in the melting mantle. [2] Objectiveness and open-mindedness (vs. "conformation bias") are requisite twins for insights and discoveries.

Acknowledgments

Author information

The author declares no conflict of interest nor competing financial interests.

References

Anderson, D.L., 2004. Simple scaling relationships in geodynamics: the role of pressure in mantle convection and plume formation. Chin. Sci. Bull. 49, 2017–2021.

Arculus, R.J., 1981. Island arc magmatism in relation to the evolution of the crust and mantle. Tectonophysics 75, 113–133.

Arculus, R.J., 1994. Aspects of magma genesis in arcs. Lithos 33, 189-208.

Armitage, J.J., Henstock, T.J., Minchull, T.A., Hoper, J.T., 2008. Modeling the composition of melts formed during continental breakup of the Southeast Greenland margin. Earth Planet Sci. Letts. 269, 248-268.

Asimow, P.D., Ghiorso, M.S., 1998. Algorithmic modifications extending MELTS to calculate subsolidus phase relations. Am. Mineral. 83, 1127-1132.

Baker, M.B., Stolper, E.M., 1994. Determination of composition of high-pressure mantle melts using diamond aggregates. Geochim. Cosmochim. Act 58, 2811-2827.

Batiza, R., Niu, Y.L., 1992. Petrology and magma chamber processes at the East Pacific Rise ~ 9°30'N. J. Geophys. Res. 97, 6779-6797.

Blundy, J.D., Cashman, K., 2005. Rapid decompression-driven crystallization recorded by melt inclusions from Mount St Helens volcano. Geology 33, 793–796.

Brodholt, J.P., Batiza, R., 1989. Global systematics of unaveraged mid-ocean ridge basalt compositions: Comments on "Global correlations of ocean ridge basalt chemistry with axial depth and crustal thickness by E,M. Klein and C.H. Langmuir". J. Geophys. Res. 94, 4231-4239.

Buiter, S., Torsvik, T.H., 2014. A review of Wilson Cycle plate margins: a role for mantle plumes in continental break-up along suture. Gondwana Res. 26, 627–653.

Campbell, I.H., 2005. Large igneous provinces and the mantle plume hypothesis. Element 1, 265-270.

Campbell, I.H., 2007. Testing the plume theory. Chem. Geol. 241, 153-176.

Campbell, I.H., Davies, G.F., 2006. Do mantle plumes exist? Episodes 29, 162–168.

Campbell, I.H., Griffiths, R.W., 1990. Implications of mantle plume structure for the evolution of flood basalts. Earth Planet. Sci. Lett. 99, 79-83.

Carmichael., I.S.E., Turner, F.J., Verhoogen, J., 1974. Igneous Petrology. New York: McGraw-Hill, 739 pp.

Cashman, K., Blundy, J.D., 2000. Degassing and crystallization of ascending andesite and dacite. Phil. Trans. R. Soc. London 358, 1487–1513.

Castillo, P.R., Natland, J.H., Niu, Y.L., Lonsdale, P., 1998. Sr, Nd, and Pb isotopic variation along the Pacific ridges from 53 to 56°S: Implications for mantle and crustal dynamic processes. Earth Planet. Sci. Lett. 154, 109-125.

Clift, P., Vannucchi, P., 2004. Controls on tectonic accretion versus erosion in subduction zones: implications for the origin and recycling of the continental crust. Rev. Geophys. 42, RG2001. doi:10.1029/2003RG000127 (31 pp.).

Coffin, M.F., Eldholm, O., 1994. Large igneous provinces: crustal structure, dimensions, and external consequences. Review of Geophysics **32**,1-36.

Condie, K.C., 2004. Supercontinents and superplume events: distinguishing signals in the geologic record. Phys. Earth Planet. Inter. 146, 319–332.

Dalton, C.A., Langmuir, C.H., Gale, A., 2014. Geophysical and geochemical evidence for deep temperature variations beneath mid-ocean ridges. Science 344, 80-83.

Davidson, J.P., Reed, W.E., Davis, P.M., 1996. Exploring Earth: An introduction to physical geology. Prentice Hall, NJ, 477pp.

Davies, D.R., Rawlinson, N., Iaffaldano, G., Campbell, I.H., 2015. Lithospheric controls on magma composition along Earth's longest continental hotspot track. Nature 525, 511–514.

Davies, J.H., Davies, D.R., 2010, Earth's surface heat flows. Solid Earth 1, 5-24.

Davies, G.F., 1999. Dynamic Earth: Plates, Plumes and Mantle Convection. Cambridge University Press, Cambridge, 460 pp.

Davies, G.F., 2005. A case for mantle plumes. Chinese Sci. Bull. 50, 1541-1554.

Davies, G.F., Richards, M.A., 1992. Mantle convection. J. Geol. 100, 151-206.

Dick, H.J.B., 1989. Abyssal peridotite, very slow spreading ridges and ocean ridge magmatism. In Saunders, A.D., Norry, M.J. (Eds.) Magmatism in the Ocean Basins, Geol. Soc. Spec. Publ., 42, 71-105.

Dick, H.J.B., Fisher, R.L., Bryan, W.B., 1984. Mineralogical variability of the uppermost mantle along mid-ocean ridges. Earth Planet. Sci. Lett. 69, 88 -106.

Dick, H.J.B., Warren, J.M., Shimizu, N., 2007. Global variations in abyssal peridotite composition II: what determines the major element MORB composition. Am. Geophys. Uni. Fall Meeting, Abstract #U21B-0417.

Dick, H.J.B., Zhou, H., 2015. Ocean rises are products of variable mantle composition, temperature and focused melting. Nature Geosci. 8, 68-74.

Duncan, R.A., Richards, M.A., 1991. Hotspots, mantle plumes, flood basalts, and true polar wander. Reviews of Geophysics **29**, 31–50.

Ekström, G. Dziewonski, A.M., 1998. The unique anisotropy of the Pacific upper mantle. Nature 394, 168–172.

Ellam, R.M., 1992. Lithospheric thickness as a control on basalt geochemistry. Geology 20, 153-156.

Elliott, T., 2003. Traces of the slab. Geophys. Monogr. 238, 23-45.

England, P., Engdahl, R., Thatcher, W., 2004. Systematic variation in the depths of slabs beneath arc volcanoes. Geophys. J. Int. 156, 377–408.

England, P., Wilkins, C., 2004. England, P., Engdahl, R., Thatcher, W., 2004. Systematic variation in the depths of slabs beneath arc volcanoes. Geophys. J. Int. 159, 1138–1154

England, P.C., Katz, R.F., 2010. Melting above the anhydrous solidus controls the location of volcanic arcs. Nature 467, 700-704.

Ernst, R.E., 2014. Large igneous provinces. Cambridge University Press, Cambridge, UK.

Falloon, T.J., Green, D.H., 1987. Anhydrous partial melting of MORB pyrolite and other peridotite compositions at 10 k bar: Implications for the origin of MORB glasses. Mineral. Petrol. 37, 181–219.

Falloon, T.J., Green, D.H., 1988. Anhydrous partial melting of peridotite from 8 to 35 kb and the petrogenesis of MORB. J. Petrol. Special Lithosphere Issue, 379-414.

Falloon, T.J., Green, D.H., Hatton, C.J., Harris, K.L., 1988. Anhydrous partial melting of a fertile and depleted peridotite from 2 to 30 kb and application to basalt petrogenesis. Journal of Petrology 29, 1257–1282, 1988.

Fischer, K.M., Ford, H.A., Abt, D.L., Rychert, G.A., 2020. The lithosphere=asthenosphere boundary. Ann. Rev. Earth Planet Sci. 38, 551-575.

Foulger, G.R., 2005. Mantle plumes: Why the current skepticism? Chinese Sci. Bull. 50, 1555-1560.

Foulger, G.R., 2010. Plates vs Plumes: A Geological Controversy. Wiley-Blackwell, 364p.

Foulger, G.R., Natland, J.H., 2003. Is ''hotspot'' volcanism a consequence of plate tectonics? Science 300, 921–922.

Gale, A., Langmuir, C.H., Dalton, C.A., 2014. The global systematics of ocean ridge basalts and their origin. J. Petrol. 55, 1051-1082.

Ghiorso, M.S., Hirschmann, M.M., Reiners, P.W., Kress III, V.C, 2002. The pMELTS: A revision of MELTS for improved calculation of phase relations and major element partitioning related to partial melting of mantle to 3 GPa. Geochem. Geophys. Geosys. 3, 1030, doi:10.1029/2001GC000217.

Gill, J.B., 1981. Oorgenic andesites and plate tectonics. Springer-Verlag, New York, 390 pp.

Gill, J., Michael, P., Woodcock, J., Dreyer, B., Ramos, F., Clague, D., Kela, J., Scott, S., Konrad, K., Stakes, D., 2016. Spatial and temporal scale of mantle enrichment at the Endeavour Segment, Juan de Fuca Ridge. J. Petrol. 57, 863-896.

Green, D.H., 1968. Origin of basaltic magmas. In Hess, H.H. (ed.) Basalts – The Poldervaar Treaties on rocks of basaltic composition, Vol. 2. J. Wiley & Son, New York, 835-962.

Green, D.H., 1971. Composition of basaltic magmas as indicators of conditions of origin: Application to oceanic volcanism. Philosophical Transaction of the Royal Society of London A268, 707–725.

Green, D.H., 1973. Experimental melting studies on a model upper mantle composition at high pressure under water-saturated and water-undersaturated conditions. Earth Planet. Sci. Lett. 19, 37-53

Green, D.H., 2015. Experimental petrology of peridotites, including effects of water and carbon on melting in the Earth's upper mantle. Phys. Chem. Miner. 42, 95-122.

Green, D.H., Falloon, T.J. 2005. Primary magmas at mid-ocean ridges, "hotspots," and other intraplate settings: Constraints on mantle potential temperature. In Foulger, G.R., Natland, J.H., Presnall, D.C., Anderson, D.L. (eds), Plates, Plumes, and Paradigms, Geol. Soc. Am. Spec. paper 388, 217-248.

Green, D.H., Falloon, T.J., 2015. Mantle-derived magmas: intraplate, hot-spots and mid-ocean ridges. Sci., Bull. 60, 1873-1900.

Green, D.H., Hibberson, W.O., Kovacs I et al. 2010. Water and its influence on the lithosphere–asthenosphere boundary. Nature 467, 448-451

Green, D.H., Ringwood, A.E., 1963. Mineral assemblage in a model mantle composition. J. Geophys. Res. 68, 937-945.

Green, D.H., Ringwood, A.E., 1964. Fractionation of basalts at high pressures. Nature 201, 1276-1279.

Green, D.H., Ringwood, A.E., 1967. The genesis of basaltic magmas. Contrib. Mineral. Petrol. 15, 103-190.

Green, D.H., Ringwood, A.E., 1970. Mineralogy or peridotite compositions under upper mantle conditions. Phys. Earth Planet. Inter. 3, 359-371.

Griffiths, R.W., Campbell, I.H., 1990. Stirring and structure in starting plumes. Earth and Planetary Science Letters 99, 66-78.

Grove, T.L., Till, C.B., Krawcybski, M.J., 2012. The role of H_2O in subduction zone magmatism. Ann, Rev. Earth Planet Sci. 40, 413-439.

Guo, P.Y., Niu, Y.L., Sun, P., Gong, H.M., Wang, X.H., 2020. Lithosphere thickness controls the continental basalt compositions: An illustration using the Cenozoic basalts from eastern China. Geology 48, 128-133.

Guo, P.Y., Niu, Y.L., Ye, L., Liu, J.J., Sun, P., Cui, H.X., Zhang, Y., Gao, J.P., Su, L., Zhao, J.X., Feng, Y.X., 2014. Lithosphere thinning beneath west North China Craton: Evidence from geochemical and Sr-Nd-Hf isotope compositions of Jining basalts. Lithos 202/203, 37-54.

Haase, K.M., 1996. The relationship between the age of the lithosphere and the composition of oceanic magmas: constraints on partial melting, mantle sources and the thermal structure of the plates. Earth Planet. Sci. Lett. 144, 75–92.

Herzberg, C, O'Hara, M.J., 2002. Plume-associated ultramafic magmas of Phanerozoic age. Journal of Petrology **43**, 1857-1883.

Herzberg, C., Asimow, P.D., Arndt, N., Niu, Y.L., Lesher, C.M., Fitton, J.G. Cheadle, M.J., Saunders, A.D., 2007. Temperatures in ambient mantle and plumes: Constraints from basalts, picrites and komatiites. Geochem. Geophys. Geosys. 8, Q02006, doi:10.1029/2006GC001390.

Hill, R.I., 1991. Starting plumes and continental break-up. Earth Planet. Sci. Lett. 104, 398–416.

Hill, R.I., Campbell, I.H., Davies, G.F., Griffiths, R.W., 1992. Mantle plumes and continental tectonics. Science 256, 186-193.

Hirose, K., Kushiro, I., 1993. Partial melting of dry peridotites at high pressures: Determination of compositions of melts segregated from peridotites using aggregates of diamonds. Earth Planet. Sci. Lett. 114, 477-489.

Hirth, G., Kohlstedt, D.L., 1996. Water in the oceanic upper mantle: implications for rheology, melt extraction and the evolution of the lithosphere. Earth Planet. Sci. Lett. 144, 93–108.

Hofmann, A.W., 1988. Chemical differentiation of the Earth: The relationship between mantle, continental crust, and oceanic crust, Earth Planet. Sci. Lett., 90, 297 – 314, 1988.

Hofmann, A.W., 1997. Mantle geochemistry: The message from oceanic volcanism, Nature, 385, 219 – 229.

Humphreys, E.R., Niu, Y.L., 2009. On the composition of ocean island basalts (OIB): The effects of lithospheric thickness variation and mantle metasomatism. Lithos 112, 118-136.

Ionov, D.A., Benard, A., Plechov, P.Yu., Sjcherbakov, V.D., 2012. Along-arc variations in lithospheric mantle compositions in Kamchatka, Russia: First trace element data on mantle xenoliths from the Klyuchevskoy Group volcanoes. Chem. Geol. 263, 122-131.

Jaques, A.L., Green, D.H., 1980. Anhydrous melting of peridotite at 0–15 kb pressure and the genesis of tholeiitic basalts. Contrib. Mineral. Petrol. 73, 287–310.

Jennings, E., Gibson, S.A., MacLennan, J., 2019. Hot primary melts and mantle source for the Parana-Etendeka flood basalt province: New constraints from Al-in-olivine thermometry. Chem. Geol. 529, 119287.

Johnson, K.T.M., Dick, H.J.B., Shimizu, N., 1990. Melting in the oceanic upper mantle: an ion microprobe study of diopsides in abyssal peridotites. J. Geophys. Res. 95, 2661–2678.

Karason, H., van der Hilst, R., 2000. Constraints on mantle convection from seismic tomography. Geophys. Monogr. 121, 277–288.

Karato, S.I., 2003. The dynamic structure of the deep earth. – Princeton University Press, Princeton, 241 p.

Kennett, B.L.N, Engdahl, E.R., 1991. Traveltimes for global earthquake location and phase identification. Geophys. J. Int. 105, 429-465.

Kinzler, R.J., Grove, T.L., 1992. Primary magmas of mid-ocean ridge basalts, 2, Applications. J. Geophys. Res. 97, 6970-6926.

Klein E.M., Langmuir, C.H., 1987. Global correlations of ocean ridge basalt chemistry with axial depth and crustal thickness. J. Geophys. Res. 92, 8089–8115.

Klein E.M., Langmuir, C.H., 1989. Local versus global variation in ocean ridge compositions: A reply. J. Geophys. Res. 94, 4241-4252.

Kushiro, I. 1968. Compositions of magmas formed by partial zone melting of the Earth's upper mantle. J. Geophys. Res. 73, 619-634

Kushiro I. 1973. Origin of some magmas in oceanic and circum-oceanic regions. Tectonophys. 17, 211-222

Langmuir, C.H., Klein, E.M., Plank, T., 1992. Petrological systematics of mid-ocean ridge basalts: Constraints on melt generation beneath ocean ridges. In Phipps Morgan, J., Blackman, D.K., Sinton, J.M. (eds.), Mantle flow and melt generation at mid-ocean ridges, Am. Geophys. Uni. Monogr. 71, 183-280.

Langmuir, C.H., Bender, J.F., Batiza, R., 1986. Petrological and tectonic segmentation of the East Pacific Rise, 5°30'–14°30'N. Nature 322, 422–429.

Larsen, H.C., Duncan, R.A., Allan, J.F., Brooks, K. (eds), 1999. Proceeding of Ocean Drilling Program, Scientific Results 163 (doi:10.2973/odp.proc.sr.163.1999), College Station, USA.

Lee, C.-T., Luffi, P., Plank, T., Dalton, H., Leeman, W.P., 2009. Constraints on the depths and temperatures of basaltic magma generation on Earth and other terrestrial planets using new thermobarometers for mafic magmas. Earth Planet. Sci. Lett. 279, 20-33.

Li, X.H., Li, W.X., Li, Z.X., Liu, Y., 2008. 850-790 Ma bimodal volcanic and intrusive rocks in northern Zhejiang, South China: A major episode of continental rift magmatism during the breakup of Rodinia. Lithos 102, 341-357.

Li, Z.X., Li, X.H., Kinny, P.D., Wang, J., 1999. The breakup of Rodinia: Did it start with a mantle plume beneath South China? Earth Planet. Sci. Lett. 173, 171–181.

Lundstrom, C.C., Gill, J., Williams, Q., Perfit, M.R., 1995. Mantle melting and basalt extraction by equilibrium porous flow. Science 270, 1958-1961.

Macdonald, K.C., 1982. Mid-ocean ridges: Fine scale tectonic, volcanic and hydrothermal processes within the plate boundary zone. Ann. Rev. Earth Planet. Sci. 10, 155-190

McDonough, W.F., Sun, S.-s, 1995. The composition of the Earth. Chem. Geol. 67, 1050-1056.

McKenzie, D., 1984. The generation and compaction of partially molten rock. J. Petrol 25, 713-765.

McKenzie, D., 1985. ^{230}Th–^{238}U disequilibrium and the melting processes beneath ridge axes. Earth Planet. Sci. Lett. 72, 81–91.

McKenzie, D., 2020. Speculations on the generation and movement of komatiites, J. Petrol. 62, doi:10.1093/petrology/egaa061.

McKenzie, D., Bickle, M.J., 1988. The volume and composition of melt generated by extension of the lithosphere. J. Petrol 29, 625–679

McKenzie, D., Daly, N.D., Priestley, K., 2015. The lithospheric structure of Pangea. Geology 43, 783-786.

McKenzie, D., Jackson, J., Priestley, K., 2005. Thermal structure of oceanic and continental lithosphere. Earth Planet Sci. Lett. 233, 227-349.

Morgan, W.J., 1971. Convection plumes in the lower mantle. Nature 82, 575-587.

Natland, J.H., 1989. Partial melting of a lithologically heterogeneous mantle: Inferences from crystallisation histories of magnesian abyssal tholeiites from the Siqueiros Fracture Zone. In Saunders, A.D., Norry, M.J. (eds) Magmatism in the Ocean Basins, Geol. Soc. Spec. Publ. 42, 41-70.

Niu, Y.L., 1992. Mid-ocean ridge magmatism: Style of mantle upwelling, partial melting, crustal level processes, and spreading rate dependence: A petrologic approach, PhD thesis, University of Hawaii, Honolulu, 250 pp.

Niu, Y.L., 1997. Mantle melting and melt extraction processes beneath ocean ridges: Evidence from abyssal peridotites. J. Petrol 38, 1047-1074.

Niu, Y.L., 2004. Bulk-rock major and trace element compositions of abyssal peridotites: Implications for mantle melting, melt extraction and post-melting processes beneath ocean ridges. J. Petrol 45, 2423-2458.

Niu, Y.L., 2005a. Generation and evolution of basaltic magmas: Some basic concepts and a hypothesis for the origin of the Mesozoic-Cenozoic volcanism in eastern China. Geol. J. China Univ. 11, 9-46.

Niu, Y.L., 2005b. On the great mantle plume debate. Chinese Sci. Bull. 50, 1537-1540.

Niu, Y.L., 2014. Geological understanding of plate tectonics: Basic concepts, illustrations, examples and new perspectives. Global Tectonics and Metallogeny 10, 23-46.

Niu, Y.L., 2016a. The meaning of global ocean ridge basalt major element compositions. J. Petrol 57, 2081-2104.

Niu, Y.L., 2016b. Testing the geologically testable hypothesis on subduction initiation. Sci. Bull. 61, 1231-1235.

Niu, Y.L., 2020a. On the cause of continental breakup: A simple analysis in terms of driving mechanisms of plate tectonics and mantle plumes. J. Asian Earth Sci. 194, 104367.

Niu, Y.L., 2020b. What drives the continued India-Asia convergence since the collision at 55 Ma? Sci. Bull. 65, 169-172.

Niu, Y.L, Green, D.H., 2018. The petrological control on the lithosphere-asthenosphere boundary (LAB) beneath ocean basins. Earth-Sci. Rev. 185, 301-307.

Niu, Y.L., Batiza, R., 1991a. An empirical method for calculating melt compositions produced beneath mid-ocean ridges: Application for axis and off-axis (seamounts) melting. J. Geophys. Res. 96, 21,753-21,777.

Niu, Y.L., Batiza, R., 1991b. In-situ densities of silicate melts and minerals as a function of temperature, pressure, and composition. J. Geol., 99, 767-775.

Niu, Y.L., Batiza, R., 1993. Chemical variation trends at fast and slow spreading ridges. J. Geophys. Res. 98, 7887-7902.

Niu, Y.L., Batiza, R., 1994. Magmatic processes at a slow spreading ridge segment: 26°S Mid-Atlantic ridge. J. Geophys. Res. 99, 19,719-19,740.

Niu, Y.L., Bideau, D., Hékinian, R., Batiza, R., 2001. Mantle compositional control on the extent of melting, crust production, gravity anomaly, ridge morphology, and ridge segmentation: a case study at the Mid-Atlantic Ridge 33 - 35°N. Earth Planet. Sci. Lett. 186, 383-399.

Niu, Y.L., Collerson, K.D., Batiza, R., Wendt, I., Regelous, M., 1999. The origin of E-type MORB at ridges far from mantle plumes: The East Pacific Rise at 11°20'N. J. Geophys. Res. 104, 7067-7087.

Niu, Y.L., Hékinian, R., 1997a. Spreading rate dependence of the extent of mantle melting beneath ocean ridges. Nature 385, 326-329.

Niu, Y.L., Hékinian, R., 1997b. Basaltic liquids and harzburgitic residues in the Garrett transform: A case study at fast spreading ridges. Earth Planet. Sci. Lett. 146, 243–258.

Niu, Y.L., Hékinian, R., 2004. Ridge suction drives plume-ridge interactions. In Hékinian, R., Stoffers, P., Cheminee, J.-L (ed.), Oceanic Hotspots, edited., Springer-Verlag, New York, p. 285-307.

Niu, Y.L., Langmuir, C.H., Kinzler, R.J., 1997. The origin of abyssal peridotites: A new perspective. Earth Planet. Sci. Lett. 152, 251-265.

Niu, Y.L., Liu, Y., Xue, Q.Q., Shao, F.L., Chen, S., Duan, M., Guo, P.Y., Gong, H.M., Hu, Y., Hu, Z.X., Kong, J.J., Li, J.Y., Liu, J.J., Sun, P., Sun, W.L., Ye, L., Xiao, Y.Y., Zhang, Y., 2015. Exotic origin of the Chinese continental shelf: New insights into the tectonic evolution of the western Pacific and eastern China since the Mesozoic. Sci. Bull. 60, 1598-1616.

Niu, Y.L., O'Hara, M.J., Pearce, J.A., 2003. Initiation of subduction zones as a consequence of lateral compositional buoyancy contrast within the lithosphere: A petrologic perspective. Journal of Petrology 44, 851-866.

Niu, Y.L., O'Hara, M.J., 2008. Global correlations of ocean ridge basalt chemistry with axial depth: A new perspective. J. Petrol. 49, 633-664.

Niu, Y.L., Regelous, M., Wendt, J.I., Batiza, R., O'Hara, M.J., 2002. Geochemistry of near-EPR seamounts: Importance of source vs. process and the origin of enriched mantle component. Earth Planet. Sci. Lett. 199, 327-345.

Niu, Y.L., Shi, X.F., Li, T.G., Wu, S.G., Sun, W.D., Zhu, R.X., 2017. Testing the mantle plume hypothesis: An IODP effort to drill into the Kamchatka-Okhotsk Sea basement. Sci. Bull. 62, 1464-1472.

Niu, Y.L., Waggoner, G., Sinton, J.M., Mahoney, J.J., 1996. Mantle source heterogeneity and melting processes beneath seafloor spreading centers: The East Pacific Rise 18° - 19°S. J. Geophys. Res. 101, 27,711-27,733

Niu, Y.L., Wilson, M., Humphreys, E.R., O'Hara, M.J., 2011. The origin of intra-plate ocean island basalts (OIB): The lid effect and its geodynamic implications. J. Petrol. 52, 1443-1468.

Niu, Y.L., Zhao, Z.D., Zhu, D.C., Mo, X.X., 2013. Continental collision zones are primary sites for net continental crust growth – A testable hypothesis. Earth-Sci. Rev. 127, 96-110.

O'Hara, M.J., 1963. Melting of garnet peridotite and eclogite at 30 kilobars. Carnegie Inst. Wash. Year Bk. 62, 71-77.

O'Hara, M.J., 1965. Primary magmas and the origin of basalts. Scot. J. Geol. 1, 18-40.

O'Hara, M.J., 1967. Crystal-liquid equilibria and the origins of ultramafic nodules in igneous rocks. In Ultramafic and Related Rocks (Ed. P.J. Wyllie) pp 346-349. J. Wiley, New York.

O'Hara, M.J., 1968a. Are ocean floor basalts primary magmas? Nature 220, 683-686.

O'Hara, M.J., 1968b. The bearing of phase equilibria studies in synthetic and natural systems on the observation of volcanic products. Earth-Sci. Rev 4, 69-133.

O'Hara, M.J., 1970. Upper mantle composition inferred from laboratory experiments and observation of volcanic products. Phys. Earth Planet. Inter 3, 236-245.

O'Hara, M.J., Yoder, Jr., H.S., 1963. Partial melting of the mantle. Yearbook, Carnegie Instit. Wash. Year Bk 62, 66-71.

O'Hara, M.J., Yoder, Jr., H.S., 1967. Formation and fractionation of basic magmas at high pressures. Sco. J. Geol. 3, 67-117.

Parkinson, I.J., Arculus, R.J., 1999. The redox state of subduction zones: Insights from arc-peridotites. Chem. Geol. 160, 409–423.

Parsons, B., McKenzie, D., 1978. Mantle convection and the thermal structure of the plates. J. Geophys. Res. 83, 4485–4496.

Parsons, B., Sclater, J.G., 1977. An analysis of the variation of ocean floor bathymetry and heat flow with age. J. Geophys. Res. 82, 803–827.

Perfit, M.R., Gust, D.A., Bence, A.E., Arculus, R.J., Taylor, S.R., 1980. Chemical characteristics of island-arc basalts: implications for mantle sources. Chem. Geol. 30, 227-256.

Perfit, M.R., Fornari, D.J., Smith, M.C., Bender, J.F., Langmuir, C.L., Haymon, R.M., 1994. Small-scale spatial and temporal variations in mid-ocean ridge crest magmatic processes. Geology 22, 375-379.

Presnall, D.C., Dixon, J.R., O'Donnell, T.H., Dixon, S.A., 1979. Generation of mid-ocean ridge tholeiites. J. Petrol. 20, 3–35.

Michael, P.J., Langmuir, C.H., Dick, H.J.B., Snow, J.E., Goldstein, S.L., Graham, D.W, 2003. Magmatic and amagmatic seafloor generation at the ultraslow-spreading Gakkel ridge, Arctic Ocean Nature 423, 956-961.

Phipps Morgan, J., 1987. Melt migration beneath mid-ocean ridge spreading centers. Geophys. Res. Lett. 14, 1238–1241.

Plank, T., Forsyth, D.W., 2016. Thermal structure and melting conditions in the mantle beneath the Basin and Range province from seismology and petrology. Geochemistry, Geophysics, Geosystems 17, 1312-1338.

Plank, T., Langmuir, C.H., 1988. An evaluation of the global variations in the major element chemistry of arc basalts. Earth Planet. Sci. Lett. 90, 349-370.

Putirka, K., 2005. Mantle potential temperatures at Hawaii, Iceland, and the mid-ocean ridge system, as inferred from olivine phenocrysts: Evidence for thermally driven mantle plumes. Geochemistry, Geophysics, Geosystems 6, Q05L08, doi:10.1029/2005GC000915.

Putirka, K., 2008. Excess temperature at ocean islands: Implications for mantle layering and convection. Geology 36, 283-286.

Regelous, M., Weinzierl, C.G., Haase, K.M., 2016. Controls on melting at spreading ridges from correlated abyssal peridotite – mid-ocean ridge basalt composition. Earth Planet. Sci. Lett. 449, 1-11.

Reid, I., Jackson, H.R., 1981. Oceanic spreading rate and crustal thickness. Mar. Geophys. Res. 5. 165-172.

Richards, M.A., Duncan, R.A., Courtillot, V., 1989. Flood basalts and hotspot tracks, plume heads and tails. Science 246, 103-107.

Ringwood, A.E. 1962. A model for the upper mantle, J. Geophys. Res. 67, 857-867.

Sager, W.W., Sano, T., Geldmacher, J., 2016. Formation and evolution of Shatsky Rise oceanic plateau: Insights from IODP Expedition 324 and recent geophysical cruises. Earth-Sci. Rev. 159, 306-336.

Saunders, A.D., Larsen, H.C., Wise, S.W., 1998. Proceeding of Ocean Drilling Program, Scientific Results 152 (doi:10.2973/odp.proc.sr.152.1998) , College Station, USA.

Saunders, A.D., Storey, M., Kent, R.W., Norry, M.J., 1992. Consequences of plume-lithosphere interaction. In Storey, B.C., Alabaster, T., Pankhurst, R.J. (eds), Magmatism and the causes of continental breakup, Geol. Soc. Spec. Publ. 68, 41-60.

Sclater, J.G., Jaupart, C., Galson, D., 1980. The heat flow through oceanic and continental crust and the heat loss of the earth. J. Geophys. Res. 18, 269–311.

Schilling, J.-G., Zajac, M., Evans, R., Jonson, T., White, W., Devine, J.D., Kingsley, T., 1983. Petrological and geochemical variations along the mid-Atlantic Ridge from 29°N to 73°N. Amer. J. Sci. 283, 510–586.

Sims, K.W.W., Goldstein, S.J., Blichert-Toft, J., Perfit, M.R., Kelemen, P., Fornari, D.J., Michael, P., Murrell, M.T., Hart, S.R., DePaolo, D.J., Ball, L., Jull, M., Bender, J., , 2002. Chemical and isotopic constraints on the generation and transport of magma beneath the East Pacific Rise. Geochim. Cosmochim. Acta 66, 3481-3504.

Sinton, J.M., Smaglik, S.M, Mahoney, J.J., Macdonald, K.C., 1991. Magmatic processes at superfast spreading mid-ocean ridges: glass compositional variations along the East Pacific Rise 13°–23°S. J. Geophys. Res. 96, 6133–6155.

Sleep, N.H., 1990. Hotspots and mantle plumes: Some phenomenology. J. Geophys. Res. 95, 6715-6736.

Sleep, N.H., 1992. Hotspot volcanism and mantle plumes. Ann. Rev. Earth Planet. Sci., 20, 19–43.

Sleep, N.H., 2011. Small-scale convection beneath oceans and continents. Chinese Sci. Bull. 56, 1292–1317.

Smith, P.M., Asimow, P.D., 2005. Adiabast_1ph: A new public front-end to the MELTS, pMELTS, and pHMELTS models. Geochem. Geophysi. Geosyst. 6, Q02004, doi:10.1029/2004GC000816.

Sparks, R.S.J., Murphy, M.D., Lejeune, A.M., Watts, R.B., Barclay, J., Young, S.R., 2000. Control on the emplacement of the andesite lava dome of the Soufrière Hills volcano, Montserrat by degassing-induced crystallization. Terra Nova 12, 14-20.

Spiegelman, M, Elliott, T., 1993. Consequences of melt transport for uranium series disequilibrium in young lavas. Earth Planet. Sci. Lett. 118, 1-20.

Stein, C.A., Stein, S., 1992. A model for the global variation in oceanic depth and heat flow with lithospheric age. Nature 359, 123–129.

Stein, S., Stein, C.A., 1996. Thermo-mechanical evolution of oceanic lithosphere: implications for the subduction processes and deep earthquakes. Am. Geophys. Uni. Monogr. 96, 1-17.

Stern, R.J., 2002. Subduction zones. Rev. Geophys. 40, 3.1-3.38

Stolper, E., Newman, S., 1994. The role of water in the petrogenesis of Mariana trough magmas. Earth Planet. Sci. Lett. 121, 293-325.

Storey, B.C., 1995. The role of mantle plumes in continental breakup: Case histories from Gondwanaland. Nature 377, 301-308.

Storey, B.C., Alabaster, T., Pankhurst, R.J. (eds), 1992. Magmatism and the causes of continental break-up, Geol. Soc. Spec. Publ. 68, London, UK.

Sun, P., Niu, Y.L., Guo, P.Y., Ye, L., Liu, J.J., Feng, Y.X., 2017. Elemental and Sr-Nd-Pb isotope geochemistry of the Cenozoic basalts in Southeast China: Insights into their mantle sources and melting processes. Lithos 272/273, 16-30.

Sun, P., Niu, Y.L., Guo, P.Y., Duan, M., Chen, S., Gong, H.M., Wang, X.H., Xiao, Y.Y., 2020a. Large iron isotope variation in the eastern Pacific mantle as a consequence of ancient low-degree melt metasomatism. Geochim. Cosmochim. Acta 286, 269-288.

Sun, P., Niu, Y.L., Guo, P.Y., Duan, M., Wang, X.H., Gong, H.M., Xiao, Y.Y., 2020b. The lithospheric thickness control on the compositional variation of continental intraplate basalts: A demonstration using the Cenozoic basalts and clinopyroxene megacrysts from eastern China. J. Geophys. Res – Solid Earth 125, e2019JB019315. doi:10.1029/2019JB019315

Sun, S.-S., McDonough, W.F., 1989. Chemical and isotopic systematics of ocean basalt: Implications for mantle composition and processes. In Saunders, A.D., Norry, M., (eds) Magmatism in the Ocean Basins. Geol. Soc. Spec. Publ., 42, 323-345.

Syracuse, E.M., Abers, G.A., 2006. Global compilation of variations in slab depth beneath arc volcanoes and implications. Geochem. Geophys. Geosyst., 7, Q05017, doi:10.1029/2005GC001045.

Syracuse, E.M., van Keken, P.E., Abers, G.A., 2010. The global rage of subduction zone thermal models. Phys. Earth Planet Int. 183, 73-90.

Tatsumi, Y., Eggins, S., 1995. Subduction zone magmatism. Blackwell Science, 231 pp.

Taylor, S.R., 1967. The origin and growth of continents. Tectonophysics 4, 17–34.

Tollan, P., M.E, O'Neill, H. St C., Hermann, J., Benedictus, Arculus, R.J., 2015. Frozen melt–rock reaction in a peridotite xenolith from sub-arc mantle recorded by diffusion of trace elements and water in olivine. Earth Planet Sci. Lett. 422, 169-181.

Turner, S.J., Langmuir, C.H., 2015a. What processes control the chemical compositions of arc front stratovolcanoes? Geochem., Geophys., Geosys. 16, 1865-1893

Turner, S.J., Langmuir, C.H., 2015b. The global chemical systematics of arc front stratovolcanoes: Evaluating the role of crust processes. Earth Planet. Sci. Lett. 422, 182-193.

Turner, S.J., Langmuir, C.H., Katz, R.F., Dungan, M.A., Stéphane, E., 2016. Parental arc magma compositions dominantly controlled by mantle-wedge thermal structure. Nat. Geosci. 9, 772-776.

Verhoogen, J., 1954. Petrological evidence on temperature distribution in the mantle of the earth. Trans. Am. Geophys. Union 35, 85-92.

Wada, I., Wang, K., 2009. Common depth of slab-mantle decoupling: reconciling diversity and uniformity of subduction zones. Geochem. Geophys. Geosyst. 10, Q10009, doi:10.1029/2009GC002570.

Wang, X.C., Li, W.X., Li, Z.X., Liu, Y., Yang, Y.H., Liang, X.R., Tu, X.L., 2008. The Bokou basalts in the northwestern Yangtze block, South China: Remnants of 820-810 Ma continental basalts. GSA Bulletin 120, 1478-1492.

Watson, S., McKenzie, D., 1991. Melt generation by plumes: A study of Hawaiian volcanism. J. Petrol. 32, 501-637.

White, R., McKenzie, D., 1989. Magmatism at rift zones: The generation of volcanic continental margins and flood basalts. J. Geophys. Res 94, 7685-7729.

White, R., McKenzie, D., 1995. Mantle plumes and flood basalts. J. Geophys. Res 100, 17543-17585.

Wilson, J.T., 1963. A possible origin of the Hawaiian Islands. Can. J. Phys. 41, 863-879.

Wyllie, P. J., 1971. The Dynamic Earth: A Textbook in Geosciences. New York: John Wiley, 416 p.

Wyllie, P. J., 1988a. Magma genesis, plate tectonics, and chemical differentiation of the Earth. Reviews of Geophysics 26, 370-404.

Wyllie, P.J., 1988b. Solidus curves, mantle plumes, and magma generation beneath Hawaii. J. Geophys. Res. 93, 4171-4181.

Yang, H.-J., Frey, F.A., Clague, D.A., 2003. Constraints on the source components of lavas forming the Hawaiian North Arch and Honolulu volcanics. Journal of Petrology 44, 603-627.

Yoder, H.S., Generation of basaltic magmas, 1976. National Academy of Science Press, Washington, D.C., 265 pp.

Zhang, N., Dang, Z., Huang, C., Li, Z.X., 2018. The dominant driving force for supercontinent breakup: plume push or subduction retreat? Geosci. Front. 9, 997–1007.

Zhong, S.J., Zhang, N., Li, Z.X., Roberts, J.H., 2007. Supercontinent cycles, true polar wander, and very long-wavelength mantle convection. Earth Planet. Sci. Lett. 261, 551–564.

Zhou, H., Dick, H.J.B., 2013. Thin crust as evidence for depleted mantle supporting the Marion Rise. Nature 494, 195-200.

Zindler, A., Hart, S.R., 1986. Chemical dynamics. Ann. Rev. Earth Planet. Sci. 14, 493-571.

Figure captions:

Fig. 1. **[a]** The familiar Earth cross section showing the internal layered structure as indicated, where 660-D and 410-D are, respectively, the seismic discontinuities at 660 km and 410 km depths, and LVZ is the seismic low velocity zone. **[b]** Seismic P-wave and S-wave velocity variation as a function of depth in the Earth's interior. The equations in **[a]** state that it is the material properties (i.e., density ρ, bulk modulus K and shear modulus μ) that determine P-wave velocity (V_P) and S-wave velocity (V_S). The figure is based on various versions in the literature using the model of Kennett and Engdahl (1991).

Fig. 2. Cartoon, modified from Davidson et al. (1996), showing major tectonic settings where mantle melting takes place to produce basaltic magmas. Plate separation along global ocean ridges (divergent plate margins) causes mantle melting to produce mid-ocean ridge basalts (MORB; e.g., East Pacific Rise) that make up the ocean crust. Subducting slab dehydration causes mantle wedge melting above subduction zones (convergent plate margins) to produce volcanic arc basalts (VAB; e.g., Mariana island arc in the western Pacific) or continent-modified "basalts" and the more evolved felsic magmas of andesitic, dacitic and hyolitic compositions (e.g., Andes in the eastern Pacific). Hot "mantle plumes" away from plate boundaries can melt to produce intra-plate ocean island basalts (OIB, e.g., Hawaiian islands). Basaltic magmatism in continental rifts is thought to be associated with "mantle plumes" or embryonic spreading centers. Back-arc spreading centers (not shown) also produce basalts (BABB) via the same way as for MORB. Non-rifting related continental basaltic volcanism is not shown here.

Fig. 3. **[a]** Schematic cross-section of oceanic upper mantle structure to show major tectonic settings of mantle melting in the context of plate tectonics (not to scale), where generally understood mechanisms of mantle melting is illustrated in pressure-temperature (P-T) space **b** – **e** (not to scale). **[b]** shows the concepts of mantle solidus, geotherms and mantle potential temperature (T_{MP}). The *mantle solidus* ($dT/dP_{[SOLIDUS]}$) is a material property and its position and topology in P-T space depends on the composition of mantle rocks, especially the effect of volatiles such as H_2O and CO_2 (see **[e]**). The *geotherm* or geothermal gradient is the temperature increase with depth in the mantle and can be understood as comprising two parts, the shallow *conductive geotherm* ($dT/dP_{[CONDUCTIVE]}$) corresponding to the lithosphere and the deep *convective geotherm*, which is also called adiabat or adiabatic gradient ($dT/dP_{[ADIABAT]}$) in the asthenosphere where small mantle temperature decrease with decreasing depth is not because of heat loss but is caused by volume expansion. The fact that $dT/dP_{[ADIABAT]} < dT/dP_{[SOLIDUS]}$ makes mantle melting possible when the adiabatically rising asthenosphere intersects the solidus. The mantle *potential temperature* (T_{MP}) refers to the surface projection of the mantle temperature along the adiabat, which is a useful concept to compare asthenospheric mantle temperature variation at a given depth between locations and between tectonic settings. For example, it is considered that the T_{MP} of the mantle that produces intra-plate OIB is related to deep-rooted "mantle plumes" and must be hotter (see **d**) than that of the normal mantle that produces MORB (see **c**; i.e., $T_{MP[hot], OIB)} > T_{MP[normal], MORB})$. **[c]** The scenario of mid-ocean ridges, where the lithosphere is thin and plate separation causes a parcel of solid mantle (e.g., the blue open star) to rise passively and begin to melt upon intersecting the solidus with the melting continuing until reaching the conductive geotherm. **[d]** The scenario of intra-plate

settings, where the lithosphere is thick and hotter rising mantle intersects the solidus at greater depth and begins to melt by decompression until reaching the LAB (lithosphere-asthenosphere boundary). [e] The scenario of subduction-zone settings, where water-dominated fluids released from the subducting/dehydrating slab to the mantle wedge change the position and topology of the mantle solidus to wet solidus, making the parcel of the mantle (the blue open star as in *b*) located above the wet-solidus to melt, which is often described as slab-dehydration induced mantle wedge melting or flex melting to produce volcanic arc basalts (VAB). Note that there have been different definitions on "lithosphere" as mechanical boundary layer of constant thickness of ~ 60 km beneath oceans and continents and another deep layer underneath as thermal boundary layer (e.g., McKenzie et al., 2005; Fischer et al., 2010), but in the context of mantle melting, the lithosphere is defined as the upper mantle above the pargasite (amphibole) dehydration solidus, which is the very lithosphere-asthenosphere boundary (e.g., Green et al., 2010; Niu and Green, 2018) and is fully consistent with half-space cooling model with its depth (L, or "lithosphere thickness") varying as a function of the lithosphere age (t) for seafloor < 70 Ma (i.e., $L \propto t^{1/2}$) due to heat loss or thermal contraction and constant for seafloor > 70 Ma (i.e., $L \approx 90$ km; e.g., Parson and McKenzie, 1978; Stein and Stein, 1996; Sleep, 2011; Niu and Green, 2018).

Fig. 4.   Model compositions (selected major elements) of mantle melts produced by decompression melting (Niu, 1997; also see Niu and O'Hara, 2008) to illustrate that the compositions of primary mantle melts vary as a function of the initial depth of melting, i.e., the depth at which the rising mantle intersects the solidus (e.g., $P_O = 25$, 20 and 15 kbar), and the increasing extent of melting as the mantle continues to rise. The decompression melting is arbitrarily stopped at 8 kbar for all three melting paths. The point is that SiO_2 (inverse; also weakly Al_2O_3 not shown), FeO (positive) and MgO (positive) of the primary melts are sensitive to pressure of melting, while CaO/Al_2O_3 (positive) and Na_2O (inverse; also TiO_2, K_2O, P_2O_5 not shown) are sensitive to the extent of melting. That is, the compositions of the erupted basalts contain the information on the extent of melting and final depth of melt equilibration, which can be extracted if the effects of shallow level melt evolution can be corrected for and if the effect of mantle source compositional variation can be properly evaluated. The decompression melting models are originally developed in 1991 (Niu and Batiza, 1991) and improved in 1997 (Niu, 1997) using mantle peridotite experimental data (Jaques and Green, 1980; Falloon and Green, 1987, 1998; Falloon et al., 1988; Hirose and Kushiro, 1993; Baker and Stolper, 1994). More complex and thermodynamics-based models such as pMELTS (Asimow and Ghiorso, 1998; Ghiorso et al., 2002; Smith and Asimow, 2005) are available, but the model data presented here are effective to capture the compositional systematics of primary mantle melts by decompression melting. See text for caveats in applying these models.

Fig. 5.   Schematic (left) and qualitative (right) illustrations of sub-ridge thermal structure with all the elements self-explained. The plate separation induced decompression melting begins when the upwelling mantle intersects the solidus at P_O (corresponding to T_O) and continues until the upwelling melting mantle reaches P_F (corresponding to T_F), the final depth of melting or melt-solid equilibration, which is the very base of the conductive ("cold") thermal boundary layer (CTBL; region ②) beneath the ridge.

Because of the buoyancy contrast, the melt (red-arrowed thin dash lines) ascends faster than the solid residue (blue-arrowed think lines). The melt is extracted to form the ocean crust and the residue contributes to the accretion of the lithospheric mantle. The latter, when tectonically exposed on the seafloor, is sampled as abyssal peridotites. The globally large mantle temperature variation of ΔT_O ($\propto \Delta P_O$) = ~ 250 K advocated by Langmuir and co-authors (Klein and Langmuir, 1987; Langmuir et al., 1992; Gale et al., 2014) is based on the use of MORB Fe_8 claimed to record the information on T_O and P_O (see Fig. 6). The claim is incorrect because during near-fractional decompression melting in the melting region ① from P_O to P_F, the 1-2% (or much less) melt in physical contact with 98-99% (or much more) solid matrix ensures effective and efficient melt-solid re-equilibration, especially for elements Si, Mg and Fe controlled by olivine, the most abundant mantle mineral. The 1000's of years of melting time ensure complete melt-solid re-equilibration that is readily achieved in 10's of hours in peridotite melting experiments. Therefore, if MORB melts indeed record pressure signature of melting, the signature must be P_F *not* P_O (Niu and O'Hara, 2008; Niu et al., 2011; Niu, 1997, 2004, 2016). This unavoidable conclusion based on objective, logical and rigorous analysis has been overlooked because readers conveniently stick to the widely referenced earlier model (Klein and Langmuir, 1987) without having thought about the experimental petrology. The plain language is as follows: [1] erupted MORB melts have no memory of P_O in terms of SiO_2, FeO and MgO, but can preserve the signature of P_F; [2] parameters such as Fe_8 has no significance in discussing T_{MP} and the claimed global ΔT_{MP} ($\propto \Delta P_o$) = ~ 250 K results from a petrologic misunderstanding (see Fig. 6); [3] the concept and conclusion rigorously illustrated here apply to mantle melting and basaltic magmatism in all tectonic settings on the earth; [4] MORB melts may not even record P_F because MORB melt, during ascent, crystallizes and adds olivine in the advanced residues in region ② as revealed from abyssal peridotites (Niu, 1997, 2004; Niu and Hékinian, 1997b; Niu et al., 1997).

Fig. 6. Cartoons and interpretations of the widely referenced model of ocean ridge mantle melting that stresses the primary control of mantle potential temperature variation (Klein and Langmuir, 1987 [KL87]; McKenzie and Bickle, 1988). By interpreting the inverse correlation of ridge segment-averaged MORB Fe_8 (FeO at MgO = 8 wt.%) with ridge depth and the positive correlation of MORB Na_8 (Na_2O at MgO = 8 wt.%) with ridge depth [*c*], KL87 states that MORB erupted at shallow ridges represent hot mantle that begins to melt deeper (high Fe_8) with higher extent of melting (low Na_8) whereas MORB erupted at deep ridges reflect cooler mantle that begins to melt shallower (low Fe_8) with lower extent of melting (high Na_8), resulting in thicker crust beneath shallow ridges than beneath deep ridges [*a,b*]. While this interpretation has been popular, [1] the assumption that decompression melting continues all the way to the Moho by ignoring the near-surface conductive cooling and [2] the misuse of MORB Fe_8 as proxy for mantle solidus depth and temperature have misguided the community on ocean ridge mantle melting (see Niu and O'Hara, 2008; Niu, 2016). See text for details.

Fig. 7. [*a*] Clinopyroxene modes in abyssal peridotites (AP), which are melting residues, plotted against Na_8 of spatially associated MORB (from Niu et al., 1997). The significant correlation between the two is apparently consistent with their interpretation that high extent of melting (low Na_8) and melt extraction (low Cpx in

AP) is associated with shallow ridges above hot mantle whereas low extent of melting (high Na_8) and melt extraction (high Cpx in AP) is associated deep ridges above cool mantle. The diagram is based on the Cpx-Na_2O data by Dick et al. (1984). The 18 localities and the data used are given in Niu et al. (1997). [b] offers an alternative interpretation that the correlation in *a* does not tell anything about the mantle temperature variation and varying extent of melting but is inherited from the sub-ridge fertile mantle compositional variation reflecting previous melting and melt extraction histories (Niu, 2004, 2016).

Fig. 8. [a] showing spreading-rate interval averaged global MORB compositions in terms of K_2O/TiO_2 and Ca_{72}/Al_{72} that vary systematically as a function of spreading rate (Niu and Hékinian, 1997a; Niu, 2016; where subscript 72 refers to corresponding oxides (wt. %) corrected for the effects of cooling-dominated crustal level processes to Mg# = 0.72 to discuss mantle processes. The heavy averaging is done to objectively examine the presence and significance of spreading rate effect if any by averaging out all other non-spreading-rate factors (e.g., effects of fertile mantle source compositional variation, including the arbitrary N- and E-type MORB division, ridge axial depth variation and uncertainties associated with correction procedures). This first order trend states clearly that the extent of sub-ridge mantle melting increases with increasing spreading rate, as explained in *b*. Note that the error bars are $\pm 1\sigma$ data variability from the mean (average), not uncertainties associated with instrumental analysis. [b] Using the concept in Fig. 5 to show that the spreading-rate dependent extent of melting is a straightforward consequence of spreading-rate controlled *lid effect*, i.e., the control of the thickness of the conductive ("cold") thermal boundary layer ② (CTBL). The average rate of mantle upwelling across the ridge is the same as the half spreading rate, so with decreasing spreading rate, mantle upwelling rate decreases and the conductive cooling to the surface penetrates to greater depth, hence the CTBL thickens and P_F deepens. As a result, the decompression melting interval $P_O – P_F$ decreases and the extent of melting $F \propto (P_O – P_F)$ decreases with decreasing spreading rate. This is the concept of the "*lid effect*" (Niu and Hékinian, 1997a; Niu et al., 2011).

Fig. 9. [a] and [b], after Niu and O'Hara (2008) and Niu (2016), showing ocean ridge axial depth interval averaged global MORB major element compositions after correction for the effects of cooling-dominated crustal level processes to Mg# = 0.72 (as in Fig. 8). The heavy averaging is done to objectively evaluate the correlations with ridge depth by averaging out all other factors (e.g., effects of fertile mantle source heterogeneity between ridges and between ocean basins, spreading-rate variation, ridge axial depth variations on ridge segment scales as well as uncertainties associated with correction procedures). The significant inter-correlations of all these petrological parameters (except for SiO_2, not shown) and their systematic correlations with ocean ridge axial depth reflect globally the first order mantle compositional variation. [c] Using the concept in Fig. 5 to understand the correlations in *a* and *b*. The ridge axial depth variation and MORB chemistry variation are two different effects of a common cause by fertile mantle compositional variation. The latter determines variation in both composition and mode of mantle mineralogy, variation of mantle density, variation of ridge axial depth, source-inherited MORB compositional variation, density-controlled variation in the maximum extent of mantle upwelling, apparent variation in the extent of melting,

and the correlated variation of MORB chemistry with ridge axial depth. The mantle compositional control is readily understood as follows. The fertile mantle source is progressively more enriched (or less depleted) from beneath shallow ridges to beneath deep ridges, pointing to increasing modal garnet, jadeite/diopside ratio in clinopyroxene, and pyroxenes/olivine ratio, thus a progressively denser mineral assemblage towards beneath deep ridges as shown in *c*. This explains in simple clarity why deep ridges are deep (enriched and dense) and shallow ridges are shallow (depleted and less dense) (see Niu and Batiza, 1991b; Niu et al., 2003) because of isostasy as quantified by Niu and O'Hara (2008). In addition, dense fertile mantle beneath deep ridges upwells reluctantly in response to plate separation, which leads to limited extent of upwelling, allowing conductive cooling to penetrate to a great depth, making a thickened cold thermal boundary layer (CTBL, region ②), forcing melting to stop at a deep level (P_F), thus having short melting interval (P_O-P_F), melting less, and producing probably a thin magmatic crust relative to the more refractory fertile mantle beneath shallow ridges. Therefore, the correlations in *a* and *b* result from the *lid effect* as illustrated in *c*.

Fig. 10. **[*a*]** Variation of average compositions of global ocean island basalt (OIB) geochemistry as a function of lithosphere thickness (*L*, the depth of the LAB below seafloor) at the time of OIB eruption (after Humphreys and Niu, 2009; Niu et al., 2011; Niu and Green, 2018). The heavy averaging was done for 10-kilometer lithosphere thickness intervals using 12,955 samples from 115 ocean islands with known seafloor ages (*t*, used to calculate $L = 11t^{1/2}$) at the time of OIB eruption from the Pacific, Atlantic and Indian oceans (see data details in Humphrey and Niu, 2009). The subscript 72 refers to corresponding oxides (SiO_2, TiO_2, Al_2O_3, FeO, MgO, CaO, P_2O_5) corrected to $Mg^{\#} = 0.72$ as in Figs. 8-9 (see Humphreys and Niu, 2009; Niu et al., 2011). **[*b*]** Illustration that the correlations in *a* are a straightforward consequence of the *lid effect*. OIB erupted on thick lithosphere have geochemical characteristics of low extent of melting (high Ti_{72}, P_{72}, $[Sm/Yb]_N$) and high pressure of melting extraction (low Si_{72}, high Mg_{72} and $[Sm/Yb]_N$), while OIB erupted on thin lithosphere exhibit the reverse. That is, the base of the lithosphere, i.e., the LAB depth (= P_F), caps the decompression melting. Hence, with increasing lithosphere thickness, P_F increases and F ($\propto P_O$-P_F) decreases, thus giving the geochemical signature of lower extent of melting and higher pressure/depth of melt extraction. This observation based understanding offers two important insights: [1] the LAB is an amphibole-dehydration solidus, above which is the conductive lithosphere (amphibole bearing peridotite) and below which is the convective asthenosphere (peridotite with incipient melt) (Niu and Green, 2018); [2] the pressure signatures in OIB records the depth of LAB (= P_F), not any deeper, which is consistent with the concept and analysis in Fig 5. The latter tells us explicitly that calculated OIB melting depths (P_O and also T_O and thus T_{MP}) that are variably and significantly deeper than the LAB using basalt-olivine-based thermobarometers have no significance; OIB compositions only record P_F at the LAB depth and have no memory of P_O and T_O because of effective and efficient melt-solid equilibration in the melting mantle, especially for elements Mg, Fe and Si controlled by olivine ($[Mg,Fe]_2SiO_4$) that is the dominant mantle mineral and is readily equilibrated with the melt as demonstrated experimentally (See Fig. 5; Niu et al., 2011; Niu, 2016). The red and green arrowed lines in the lower right panels are the adiabat of the melting mantle.

Fig. 11. [*a*] Arc-averaged compositions of modern global volcanic arc basalts (VAB) above subduction zones show significant correlations with crustal thickness (adapted from Turner and Langmuir, 2015a,b) as recognized previously using limited dataset (Plank and Langmuir, 1988). The subscript 6.0 refers to values corrected to MgO = 6.0 wt.%. In reproducing these plots, I color-code the data separating arcs built on oceanic (blue) and continent (purple) basement (Clift and Vannucchi, 2004; Syracuse et al., 2010). The authors argue that these correlations are not caused by crustal level processes but reflect mantle melting processes and the extent of mantle wedge melting increases with decreasing crustal thickness. [*b,c*] Among alternative interpretations, the authors (Turner and Langmuir, 2015a) seem to show their preference for the possible effect of the lithosphere thickness on the extent of mantle wedge melting and VAB chemistry by assuming the arc crustal thickness in *a* as a proxy for lithosphere thickness without elaboration, yet emphasize in [*d*] that mantle wedge temperature structure exerts the primary control on the extent of mantle wedge melting, where hot mantle wedge (scenario A) is argued to be associated with thin lithosphere whereas cold mantle wedge (Scenario B) is associated with thick lithosphere with globally between-wedge temperature variation of up to 250 K with respect to the dry solidus. I acknowledge the importance of the observations (*a*) but stress that the interpretation (*d*) is problematic (see text).

[*e,f*] illustrates my understanding in P-T space, the *lid effect*, that is consistent with the observation (*a*), petrological concepts and geodynamic likelihood. The initial depth of mantle wedge melting takes place right below active arc volcanoes some distance above the slab surface controlled by the interplay of slab-derived fluids, mantle potential temperature and thermal effect of the subducting slab (or slab thermal parameter). The mantle wedge melting is best understood as flux-melting, diapir formation, diapiric upwelling and decompression melting. [1] The slab-derived fluids define the wet mantle wedge solidus (also see Fig. 14); [2] initial wet melting facilitates the development of diapirs; [3] buoyancy-driven rise and growth of diapirs; [4] diapiric upwelling and decompression melting; [5] decompression melting stops when capped at the LAB, the base of the conductive lithospheric lid. Hence, lithospheric thickness variation, the *lid effect*, exerts the primary control on the extent of mantle wedge melting and VAB composition (Fig. 11a). We should note that at ocean ridges, plate separation induces passive mantle upwelling and decompression melting, but in the mantle wedge, slab-dehydration induces flex-melting develops into buoyant and growing diapirs that rise and melt by decompression, which is well captured by the lithospheric *lid effect*. Note that the diapiric decompression melting mantle is likely to have steeper $dT/dP_{[ADIABAT]}$ than shown because the melt has higher heat capacity than the solid phases. The illustration in *e* and *f* can be improved when more data become available. T_{AL} stands for arc lithosphere thickness.

Fig. 12. [*a*] Portion of the world topographic map highlighting continental China and the adjacent regions with vectors of plate motion (generated from UNAVCO: http://jules.unavco.org/Voyager/GEM_GSRM). The white dashed line is the East-West great gradient line (GGL) marked by contrasting differences in elevation, gravity anomaly, crustal thickness and mantle seismic velocity from high plateaus in the west to hilly low plains of eastern China, which is the manifestation of varying lithosphere thickness from ≥ 150 km thick beneath the plateaus in the west to ≤ 80 km thick beneath eastern China (Niu 2005a). The small rectangle labelled with arrowed line **A** in white across the GGL is the study area by Guo et al. (2020) to

illustrate the *lid effect* on the Cenozoic alkali basalts detailed in Fig. 13a. The red triangles indicated with **B** are Cenozoic alkali basalt suites studied by Sun et al. (2020b) to demonstrate the *lid effect* detailed in Fig. 13b. [**b**] Global mantle seismic tomography at depths of 100 km and 150 km (Ekström and Dziewonski, 1998; Several recent global tomography models are available, but this old one is effective in illustrating the global shallow mantle seismic structure) to show that the seismic velocity anomalies beneath eastern continental China coincides with the E-W GGL in *a* (purple lines with arrow) and that the upper mantle beneath the entire eastern China resembles that of younger oceanic upper mantle with a seismic low velocity zone (LVZ) interpreted to result from introduction of water released from the Pacific slab stagnant in the mantle transition zone beneath the region (Niu, 2005, 2014), which is also responsible for the widespread alkali basalt magmatism in eastern China (Niu, 2005a, 2014; Niu et al., 2015). [**c**] Cartoon interpreting *a* that the lithosphere is thick beneath the high plateaus in western China, but thin in eastern China across the sharp GGL. Western Pacific subduction induced corner flow requires asthenospheric material replenishment from the west (i.e., remote mantle wedge suction). In response, the eastward asthenospheric flow beneath eastern China, in turn, requires material replenishment from the west beneath the plateaus. This eastward asthenospheric flow experiences decompression melting, which explains the widespread Cenozoic alkali basalt volcanism in eastern China (e.g., Sun et al., 2020b). The western Pacific trench retreat causes eastward continental drift of Eurasia and continental extension in eastern China, which can also facilitate localized decompression melting for the Cenozoic alkali basalt volcanism in eastern China (Niu, 2014). We note that the transition-zone slab released water in the form of incipient hydrous melt percolates upwards and metasomatizes the upper mantle, contributing to the source of the alkali basalts widespread in eastern China (Niu, 2005; Guo et al., 2014; Sun et al., 2017).

Fig. 13. [**a**] Plots of average compositions of Cenozoic alkali basalts of three lava fields across the GGL from locations in the rectangle **A** in Fig. 12a. In a spatial stretch of ~ 250 km from southeast to northwest across the GGL, the elevation increases from ~ 600 m to ~ 1400 m above sea level, corresponding to lithosphere thickness (the LAB depth) increase from ~ 80 km to ~ 120 km (Guo et al., 2020). The systematic variation of the petrological parameters as a function of relative distance from southeast to northwest is a simple manifestation of the *lid effect*, i.e., increasing pressure/depth of melt extraction (decreasing Si_{72} and increasing Mg_{72}, Fe_{72}, $[Sm/Yb]_N$) and decreasing extent of melting (increasing Ti_{72}, P_{72}, K_{72}, $[La/Sm]_N$ and $[Sm/Yb]_N$) from beneath thin lithosphere to beneath thick lithosphere. [**b**] Compositional systematics of the 10 suites of Cenozoic alkali basalts containing clinopyroxene metacysts from eastern China with a north-south spatial coverage in excess of 2,500 km (localities labeled as **B** in Fig. 12a), plotted as a function of crystallization pressure of clinopyroxene megacrysts, which is best understood as crystallized from a "stable magma reservoir" close beneath the LAB (Sun et al., 2020b). These systematics are manifestations of the *lid effect*, i.e., with increasing pressure of clinopyroxene megacryst crystallization (i.e., the LAB depth), the compositions of the melt indicate increasing pressure of melt extraction (decreasing Si_{72} and Al_{72}, and increasing Fe_{72}, Mg_{72} and $[Sm/Yb]_N$) and decreasing extent of melting (increasing Ti_{72}, P_{72}, $[Sm/Yb]_N$). The strength of the garnet signature, as predicted, increases with increasing pressure (increasing $[Sm/Yb]_N$ and decreasing Sc) because Sc and Yb are highly compatible in garnet. The definition of the parameters

is the same as in Figs. 8-10).

Fig. 14. **[a]** The idea of mantle plume initiation at the core-mantle boundary (CMB), its rise and growth into a spherical plume head, the flattening and impact of the plume head upon reaching the lithosphere and beginning to melt by decompression (Campbell and Griffiths, 1990; Campbell, 2005; figure after Saunders et al., 1992). **[b]** An advanced scenario presented and described by Campbell (2007) as follows. A plume head of ~ 1000 km diameter rises beneath continental crust, flattens and melts by decompression to form a flood basalt province. Arrival of the plume head also leads to uplift, which places the lithosphere under tension, as shown by the arrows. The final diameter of the flattened plume head is claimed to reach 2000-2500 km. Tension introduced by the plume head can lead to run-away extension and the formation of a new ocean basin, drawing the hot plume head into the spreading center leading to the formation of thickened oceanic crust represented by the seaward dipping (seismic) reflectors (SWDRs) as seen on both sides of the North Atlantic genetically associated with the Iceland plume (White and McKenzie, 1989; Saunders et al., 1998; Larsen et al., 1999) and many other passive continental margins (Storey et al., 1992; Coffin and Eldholm, 1994; Ernst, 2014). **[c]** Modified after Niu (2020) and Niu et al. (2015) (with the wet solidus and dehydration solidus adapted from Green et al. (2010) and Green (2015), showing in P-T space the mantle solidus (McKenzie and Bickle, 1988) and adiabat for two scenarios with $T_{MP} = 1600°C$ for mantle plumes of dynamic upwelling and $T_{MP} = 1350°C$ appropriate for passive upwelling beneath ocean ridges for comparison. To illustrate the concept, I choose $T_P = 1600°C$ for the plume scenario, which is probably hotter than widely assumed. In the lower T and P potion (upper left) are wet solidus and dehydration solidus relevant to mantle wedge melting (Fig. 11) and lithosphere-asthenosphere boundary (LAB) phase equilibria beneath ocean basins and thinned continental lithosphere with a seismic low velocity (LVZ) (Fig. 10, 12,13). **[d]** Showing three scenarios of varying thickness of continental lithosphere when impacted by a rising mantle plume head (after Niu, 2020). The inevitable conclusions are: [1] mantle plumes cannot melt by decompression to produce LIPs beneath thickened cratonic lithospheric lid; [2] LIPs in the geological record indicate thin lithosphere at the time of volcanism; [3] it is the size, thickness and strength of the continental lithosphere that determines whether a mantle plume can surface and whether a mantle plume can break up the continents, not the other way around; [4] if there are/were many more mantle plumes and plume heads beneath continents at present and probably also in Earth's history, only those arriving beneath thin or thinned lithosphere could surface through basaltic magmatism. Therefore, arrival of mantle plume heads beneath stable continents will not thin, weaken and break lithosphere, but is predicted to thicken the lithosphere and may thus be an important mechanism to cause craton stabilization (Niu, 2020).

Author information

The author declares no conflict of interest nor competing financial interests.

Highlights

- First order compositional systematics of mid-ocean ridge basalts (MORB), volcanic arc basalts (VAB), ocean island basalts (OIB) and basalts in continental interiors (CIB) vary a function of lithosphere thickness
- In all settings, lithospheric thickness controls the extent of mantle melting, depth of melt extraction and basalt compositions, i.e., the *lid effect*
- Basalts have no memory of initial depth of mantle melting, at least for olivine making elements (i.e., Si, Mg and Fe), because of effective and efficient melt-solid equilibration in the decompression melting mantle
- Thermobarometers using basalt-olivine equilibria provide no information on initial depth of melting and mantle potential temperature, but record the depth of melt extraction at the base of the *lithospheric lid*
- The strength and thickness of lithosphere controls whether a mantle plume can surface or not and large igneous provinces (LIPs) manifest thin or thinned lithosphere at the time of volcanism
- The *paradigm* of mantle potential temperature control on basalt composition needs revision
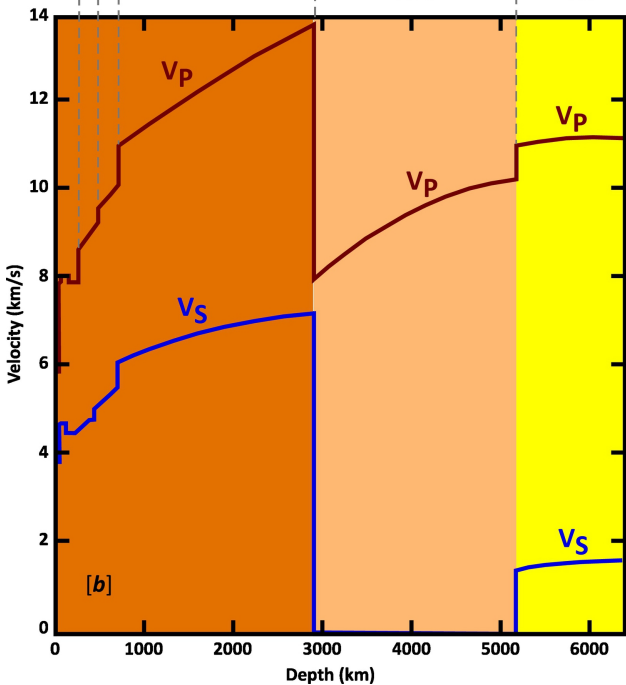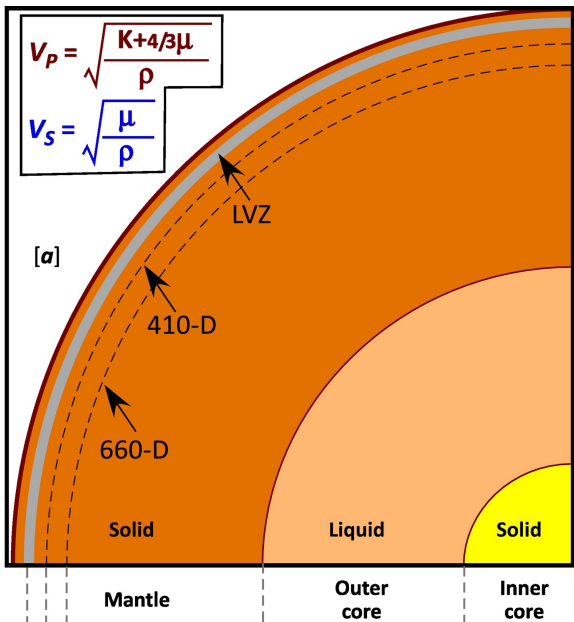
$$V_P = \sqrt{\frac{K + 4/3\mu}{\rho}}$$

$$V_S = \sqrt{\frac{\mu}{\rho}}$$

[a]

LVZ

410-D

660-D

Solid   Liquid   Solid

Mantle   Outer core   Inner core

V_P

V_S

V_P

V_P

V_S

[b]

Velocity (km/s)

Depth (km)

Figure 1

Figure 2

Figure 3

Figure 4

② Conductive thermal boundary layer (CTBL)

advanced residues

① Fertile mantle under decompression melting (P_O-P_F)

Pressure signature in MORB is P_F (variably < P_F), *not* P_o. 1-2% melt in the 98-99% solid matrix ensures effective and efficient re-equilibration, at least for olivine-making elements Si, Fe and Mg. The 1000's of years of melting time ensures complete re-equilibration as readily done in 10's of hours in peridotite melting experiments.

Upwelling rate = half-spreading rate, ~ 10 to 80 mm/year globally
With spreading rate ↓, CTBL thickens, P_F deepens, (P_O-P_F) ↓, melting extent ↓
All these have no effect on P_O!

Temperature

T_F T_O

Conductive

P_F, Final Depth of Melting

Solidus

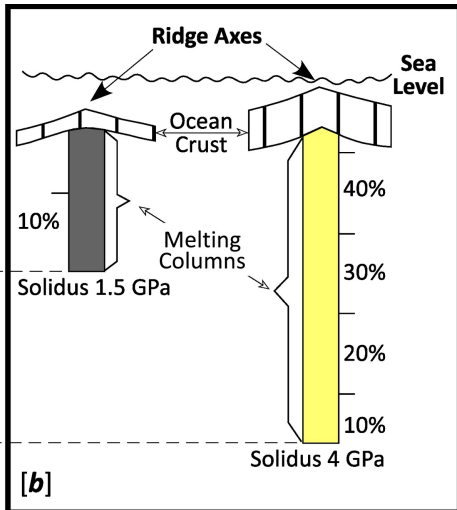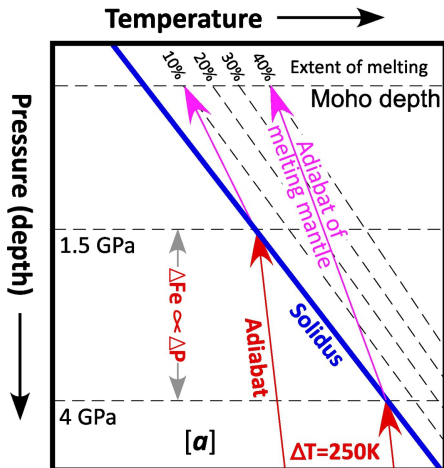P_O, Initial Depth of Melting

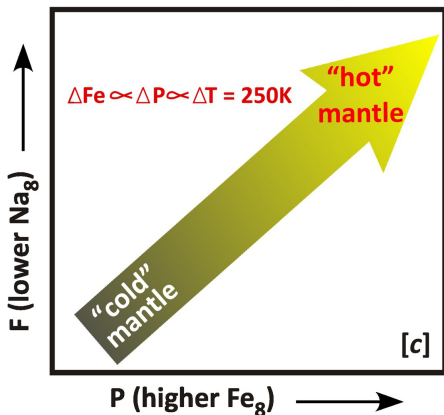**Adiabat**

Pressure

② P_F
① P_O

This concept applies to all settings: erupted basalts have no memory of P_O (thus no T_O and T_{MP} information), but can preserve P_F.
Note: MORB record P_F or variably less because of melt cooling during transport in the CTBL recorded in abyssal peridotites.

Figure 5

Klein & Langmuir (1987)

[a] Temperature → ; Pressure (depth) ↓ ; 10% 20% 30% 40% Extent of melting; Moho depth; Adiabat of melting mantle; 1.5 GPa; $\Delta Fe \propto \Delta P$; Adiabat; Solidus; 4 GPa; $\Delta T=250K$

[b] Ridge Axes; Sea Level; Ocean Crust; 10%; Melting Columns; Solidus 1.5 GPa; 40% 30% 20% 10%; Solidus 4 GPa

[c] Ridge axis shallows →; F (lower Na_8) ↑; $\Delta Fe \propto \Delta P \propto \Delta T = 250K$; "hot" mantle; "cold" mantle; P (higher Fe_8) →

The illustration is interesting, but it is **incorrect** to emphasize decompression melting continues all the way up to the base of the crust (Moho) by ignoring the conductive thermal boundary layer [CTBL] atop the mantle.

The interpretation of large variation in the initial depth of melting caused by large mantle potential temperature variation of $\Delta T_{MP}=250K$ is is **misguiding**. It is derived from MORB Fe_8 (FeO at MgO = 8 wt%) that is **invalid** to infer mantle processes:

$$P_O = 6.11 Fe_8 - 34.5 \text{ (kbar)}$$
$$T_O = 1150 + 13 \times P_O \text{ (°C)}$$
$$T_{MP} = T_O - P_O \times 1.8 \text{ (°C)}$$

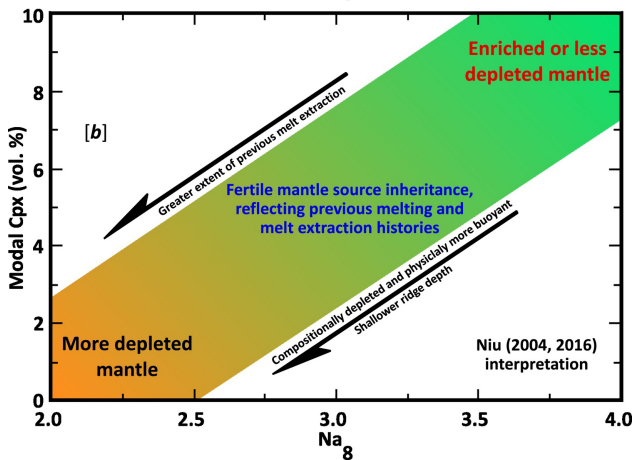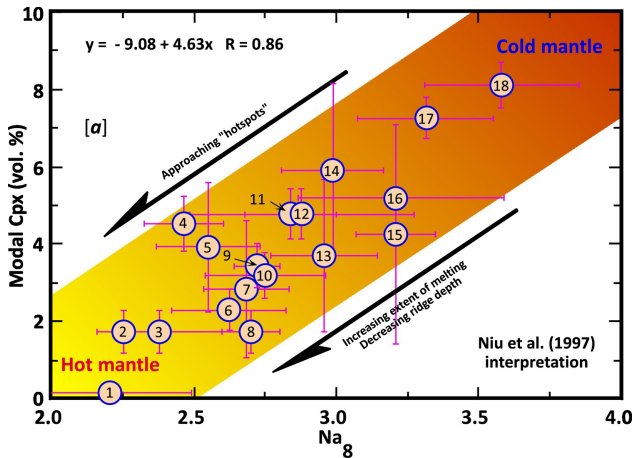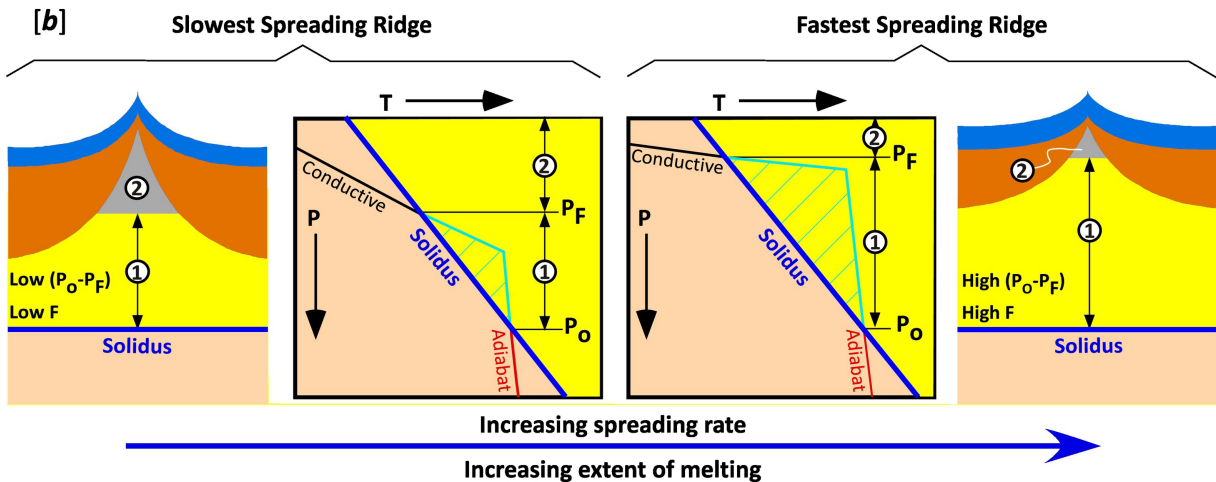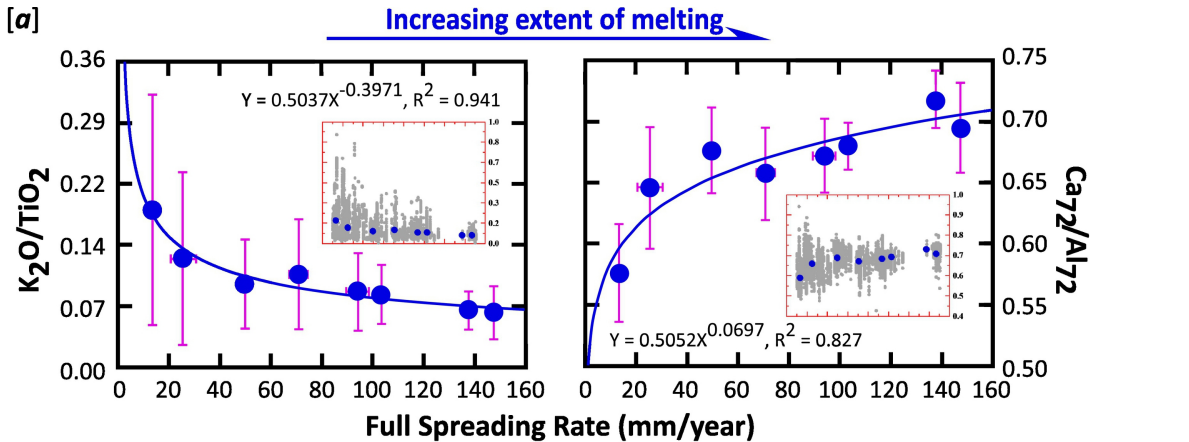All these are based on the single invalid parameter Fe_8.

Figure 6

Figure 7

[a] Increasing extent of melting

$Y = 0.5037X^{-0.3971}$, $R^2 = 0.941$

$Y = 0.5052X^{0.0697}$, $R^2 = 0.827$

K_2O/TiO_2

Ca_{72}/Al_{72}

Full Spreading Rate (mm/year)

[b] Slowest Spreading Ridge   Fastest Spreading Ridge

Low (P_O-P_F)
Low F

High (P_O-P_F)
High F

Increasing spreading rate
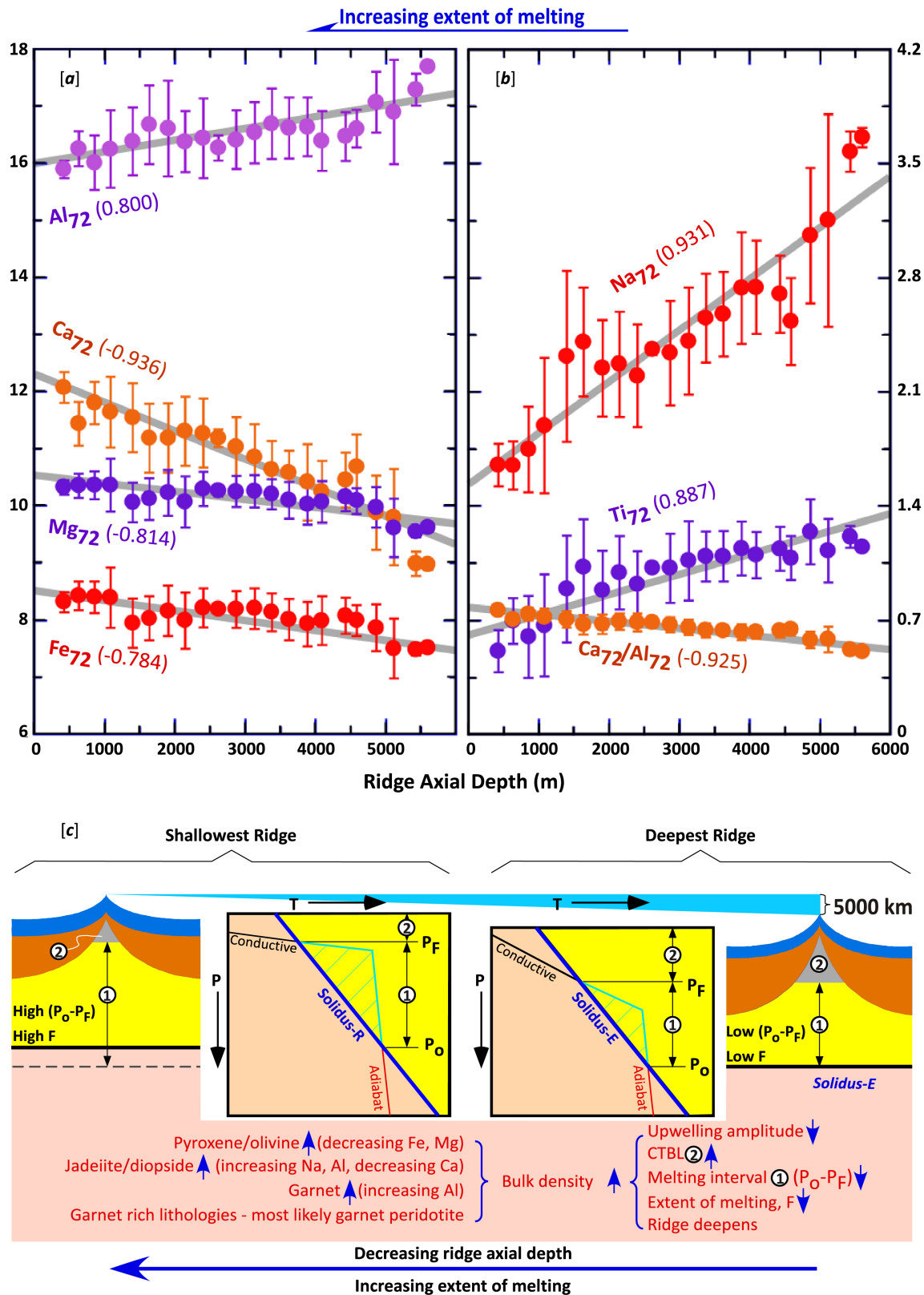
Increasing extent of melting
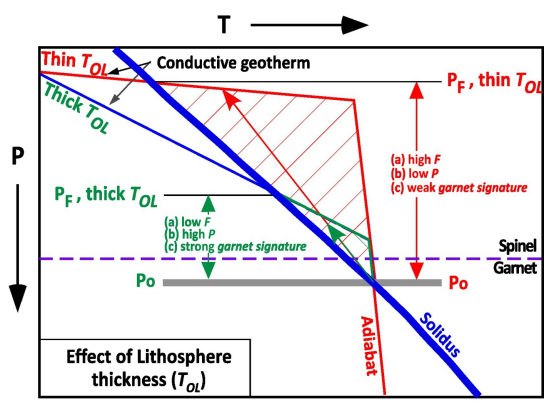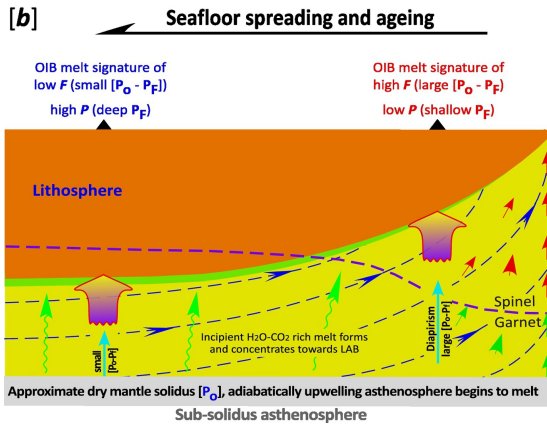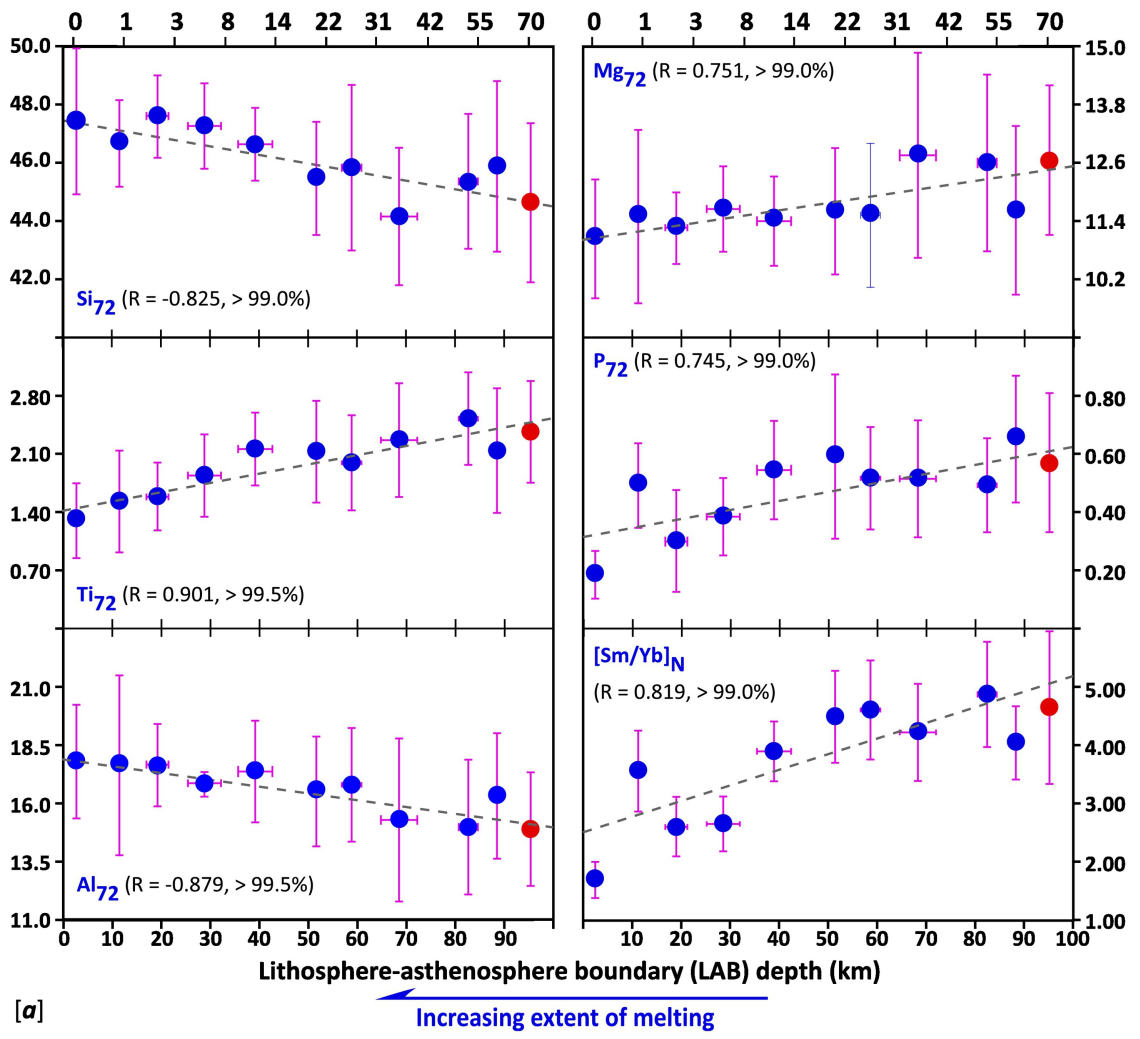
Figure 8

Figure 9

Figure 10

Increasing extent of melting

Oceanic crust 19.2±2.8 km   Continental crust 36.9±8.3 km
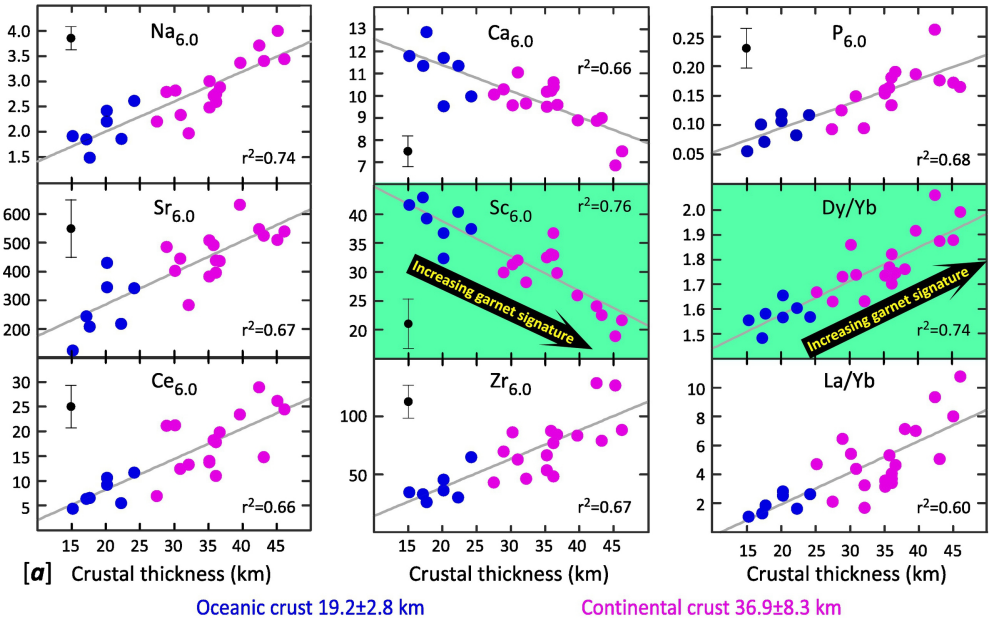
[b - d]: Turner and Langmuir (2015a) interpretation
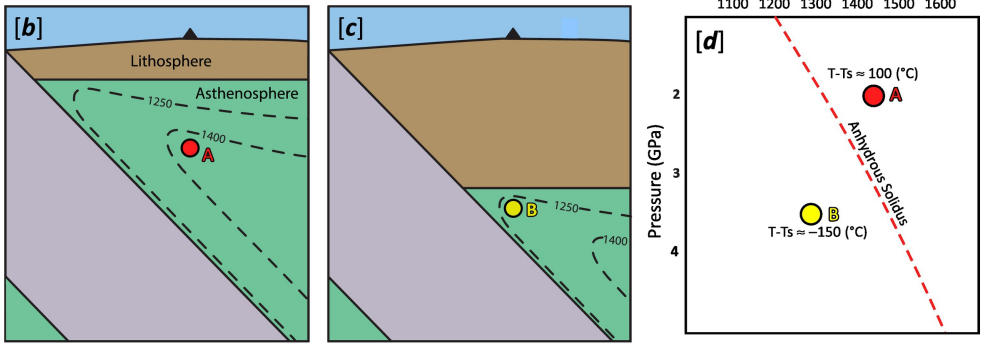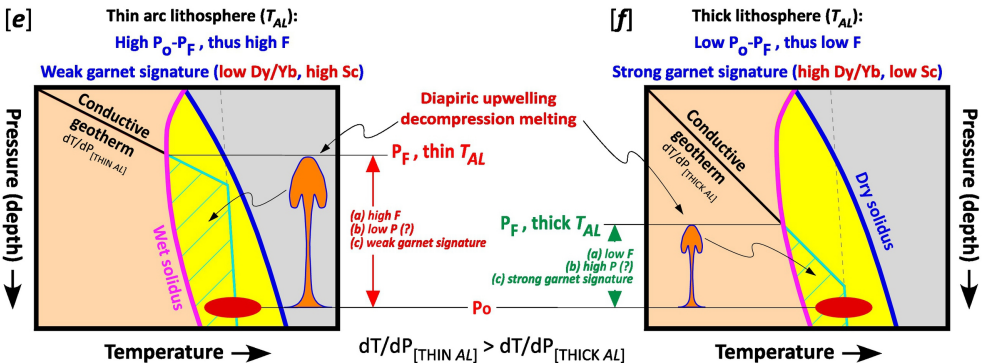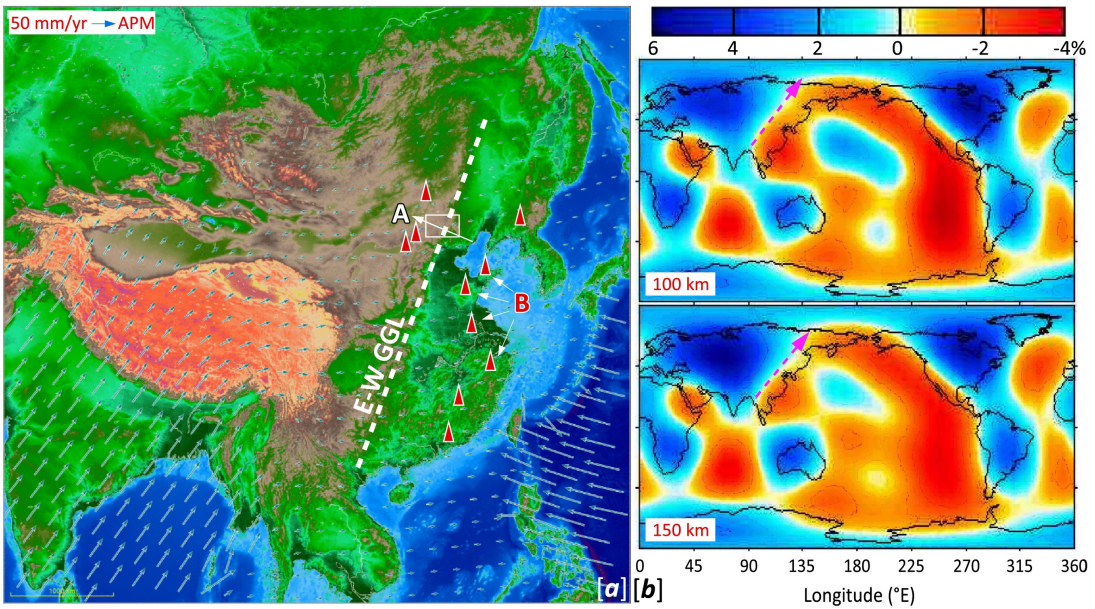
[e - f]: Understanding of this study

Figure 11

[a] [b]

[c] Origin of Cenozoic basalts in eastern continental China (see [a])

GGL: Steep gradient in elevation, morphology, crustal thickness, gravity anomaly and heat flow - all resulting from sudden lithosphere thickness change - the ISOSTATIC EFFECT

West China Plateau

East China lowland/plain

OIB-like Cenozoic basalts highly enriched in incompatible elements, but isotopically depleted with $\varepsilon_{Nd} > 0$

Lithosphere

> 150 km

< 80 km

Two causes related to western Pacific subduction:
[1] Trench retreat induced eastward continental drift and localized extension;
[2] mantle wedge suction and asthenospheric supply

Vertical component (decompression)

Actual asthenospheric flow

Remote wedge suction

Region of asthenospheric flow with decompression component, and thus decompression melting for Cenozoic volcanism

Water and hydrous melt resulting from dehydration of the stagnant Pacific slab lying horizontally in the 410D-660D mantle transition zone
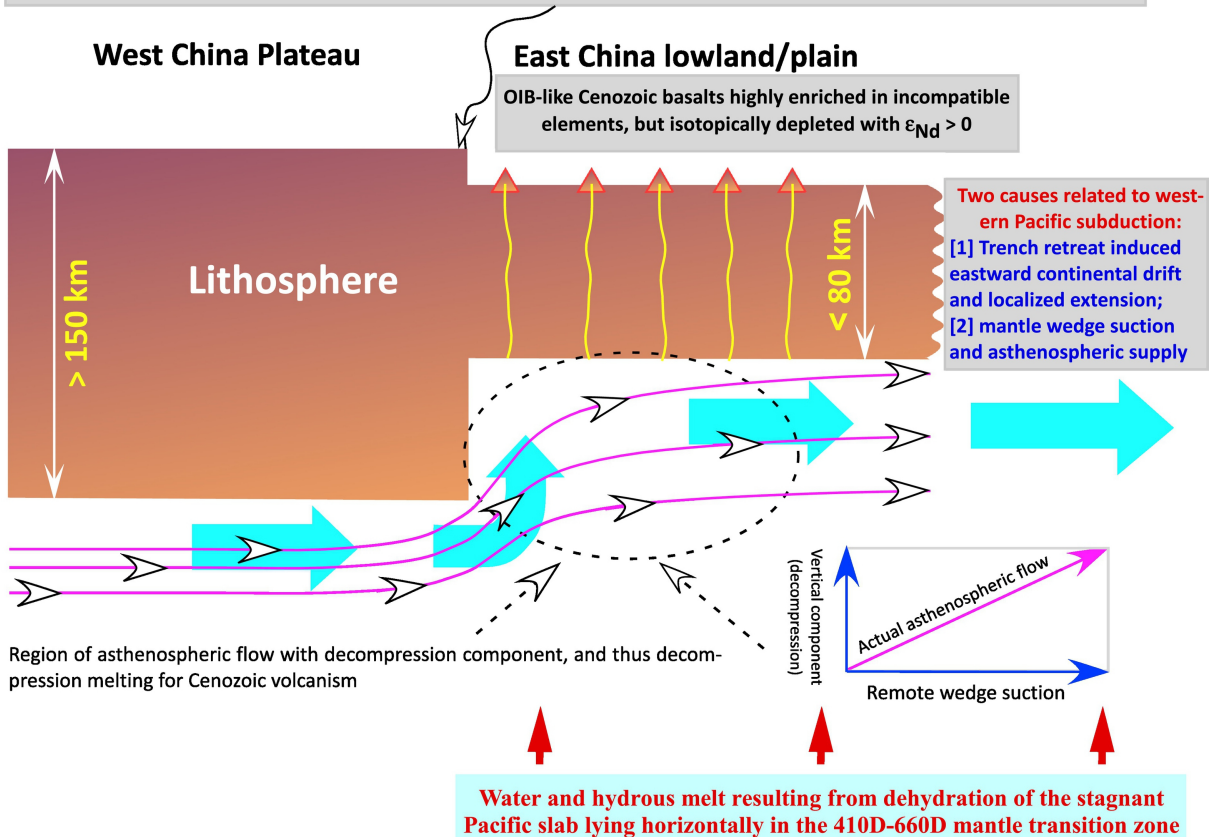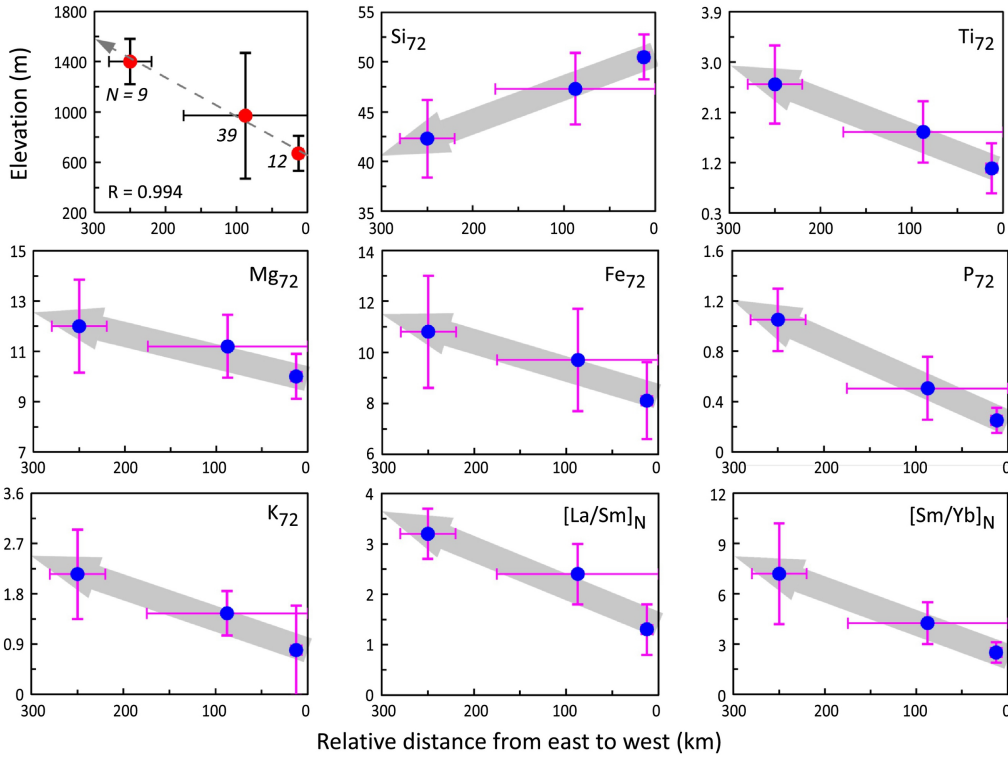
Figure 12

[a] Compositional systematics of Cenozoic basalts across the GGL along the traverse 𝔸 in Fig. 12 [a], showing the *lid effect*

Increasing topographic elevation
Increasing lithosphere thickness (from ~ 80 km to ~ 120 km)
Increasing depth (pressure) of melt extraction
Decreasing extent of melting

Relative distance from east to west (km)

[b] Compositional systematics of Cenozoic basalts as a function of final equilibration pressures recorded in the contained clinopyroxene megacrysts, showing the *lid effect* (locations indicated as 𝔹 in Fig. 12 [a])

Increasing final depth of melt equilibration at the LAB
i.e., increasing depth (pressure) of melt extraction
Increasing garnet signature
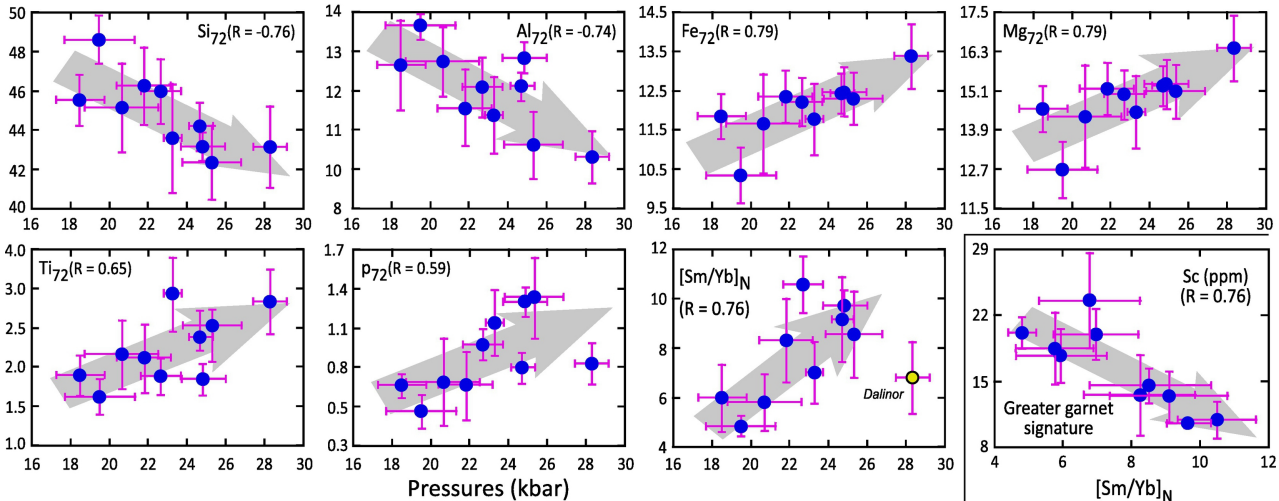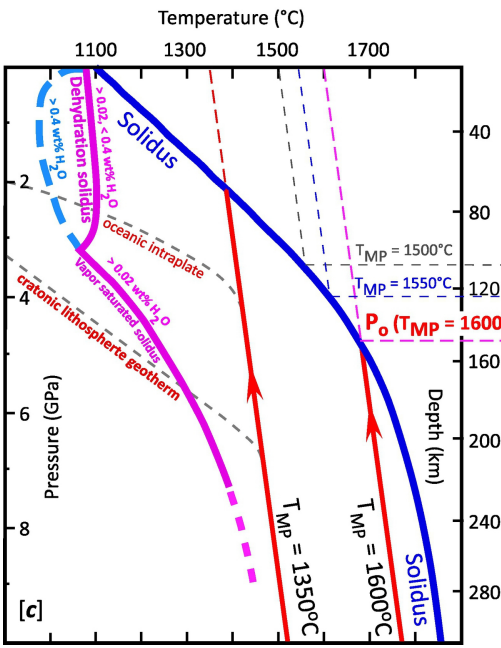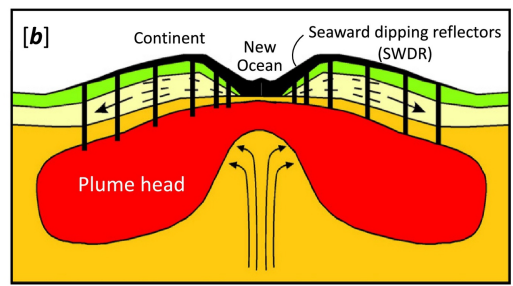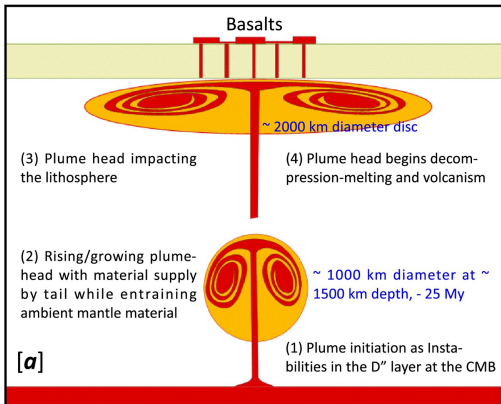Decreasing extent of melting

Pressures (kbar)

Figure 13

[a] Basalts

~ 2000 km diameter disc

(3) Plume head impacting the lithosphere

(4) Plume head begins decompression-melting and volcanism

(2) Rising/growing plume-head with material supply by tail while entraining ambient mantle material

~ 1000 km diameter at ~ 1500 km depth, ~ 25 My

(1) Plume initiation as Instabilities in the D" layer at the CMB

[b] Continent   New Ocean   Seaward dipping reflectors (SWDR)

Plume head

[c]

Temperature (°C)

1100   1300   1500   1700

Dehydration solidus
> 0.4 wt% H_2O
> 0.02, < 0.4 wt% H_2O
Solidus
oceanic intraplate
Vapor saturated solidus
> 0.02 wt% H_2O
cratonic lithosphere geotherm

T_{MP} = 1500°C
T_{MP} = 1550°C
P_0 (T_{MP} = 1600°C)

T_{MP} = 1350°C
T_{MP} = 1600°C
Solidus

Pressure (GPa)   2   4   6   8

Depth (km)   40   80   120   160   200   240   280

Rising plume head impinging the continental lithosphere

[I]
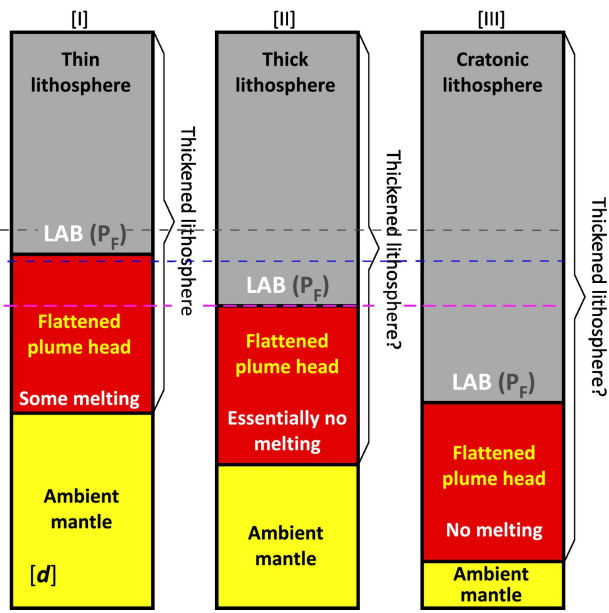Thin lithosphere
LAB (P_F)
Flattened plume head
Some melting
Ambient mantle
[d]

Thickened lithosphere

[II]
Thick lithosphere
LAB (P_F)
Flattened plume head
Essentially no melting
Ambient mantle

Thickened lithosphere?

[III]
Cratonic lithosphere
LAB (P_F)
Flattened plume head
No melting
Ambient mantle

Thickened lithosphere?

Figure 14